Investigation of Tissue Engineering Scaffolds for Potential Medical Applications

Ph.D. Thesis

Dr. Ádám Kornél Zsedényi, DDS

Supervisors:
Prof. Dr. Katalin Nagy, DDS, Ph.D.
Dr. Krisztina Buzás, Ph.D.

University of Szeged
Faculty of Dentistry
Szeged, Hungary

2017

Table of contents

TABLE OF CONTENTS **2**

LIST OF THE PUBLICATIONS: **3**

ABBREVIATIONS: **4**

I. INTRODUCTION **5**

II. OBJECTIVES **12**

III. MATERIALS AND METHODS **13**

III.1 BIODEGRADABLE POLYMER SCAFFOLDS 13
III.2 BIOLOGICAL TESTING 18
III.2.1. Tested scaffold types *18*
III.2.2. Preparation of scaffolds *18*
III.2.3. Cell types and culture condition *18*
III.2.4. In vitro experimental set-up *20*
III.2.5 In vivo experimental set-up *20*
III.2.5.1. Cytokine and chemokine proteome profiler *21*
III.2.5.2. Histology *21*
III.2.5.3 FISH *22*

IV. RESULTS **23**

V. DISCUSSION **31**

VI. CONCLUSION **33**

VII. ACKNOWLEDGMENTS **34**

VIII. REFERENCES: **35**

IX. APPENDIX **38**

List of the publications:

- **Providing the basis of the thesis:**

1. Excimer Laser-produced Biodegradable Photopolymer Scaffolds Do Not Induce Immune Rejection In Vivo

Balazs Farkas*, **Adam Zsedenyi*,** Edina Gyukity-Sebestyen, Ilaria Romano, Katalin Nagy, Alberto Diaspro, Fernando Brandi, Krisztina Buzas and Szabolcs Beke *JLMN-Journal of Laser Micro/Nanoengineering Vol. 10, No. 1, 2015* **IF:0.66** (2015) **Q2**

*Equally contribution

2. Gold nanoparticle-filled biodegradable photopolymer scaffolds induced muscle remodeling: in vitro and in vivo findings

Adam Zsedenyi, Balazs Farkas, Gaser N. Abdelrasoul, Ilaria Romano, Edina Gyukity-Sebestyen, Katalin Nagy, Maria Harmati, Gabriella Dobra, Sandor Kormondi, Gabor Decsi, Istvan Balazs Nemeth, Alberto Diaspro, Fernando Brandi, Szabolcs Beke, Krisztina Buzas

Materials Science Engineering C Materials for Biological Applications 72, 625-630.2016 Dec 02

IF: 3.420 (2016) **Q1**

- **Further publications:**

3. Role of epigenetics in EBV regulation and pathogenesis

Niller, H. H., Tarnai, Z., Decsi, G., **Zsedényi, Á**., Bánáti, F., & Minarovits, J. (2014).

Future microbiology, 9(6), 747-756

IF: 3.374 (2014)**, Q1**

Cumulative Impact Factor: 7.454

Abbreviations:

- ASC - Adipose tissue-derived Stromal/Stem Cells
- Au NP – gold NanoParticles
- BBM - Bovine Bone Mineral
- BMSC - Bone marrow Mesenchymal Stromal/Stem Cells
- CCD - Charge-Coupled Device
- DNA – DezoxyriboNucleic Acid
- ECACC - European Collection of Authenticated Cell Cultures
- EMEM - Eagle's Minimum Essential Medium
- FISH - Fluorescence *In Situ* Hybridization
- $HAuCl_4.3H_2O$ - hydrogen tetrachloroaurate trihydrates
- ICP-OES - Inductively Coupled Plasma Optical Emission Spectrometry
- IIT – Italian Institute of Technology
- LML - Laser Micromachining Laboratory
- MPExSL - Mask Projection Excimer laser StereoLithography
- MSC – Mesenchymal Stem Cell
- NP – NanoParticles
- PCL – PolyCaproLacton
- PGA - Poly(Glycolic Acid)
- HA - HydroxyApatite
- PLGA - Poly(lactic-co-glycolic) acid
- PLLA - Poly (L-lactic acid)
- PPF:DEF – Poly(Propylene-Fumarate):Diethylene Fumarate
- PVP – PolyVinylPyrrolidone
- RP - Rapid Prototyping
- SEM – Scanning Electron Microscopy
- STL - StereoLithography
- TE- Tissue Engineering

I. Introduction

Regenerative medicine seeks to create functional tissues to recover lost tissue or organ functions. Such loss can stem from various conditions that hamper the patient's quality of life, including disease and aging, but congenital diseases, where the function is not lost, but originally missing, also belong here. The field of regenerative medicine is evolving rapidly, and bears the promise of new, more individualized therapies with fewer side effects and complications [1].

The term itself is considered to have been coined by William Heseltine, who meant 'the broad range of disciplines adopted by companies working towards a common goal of replacing or repairing damaged or diseased tissue' by it. In this sense, 'regenerative medicine' is an umbrella term that covers a wide range of methods and interventions, from tissue engineering (TE), through stem cell therapy to therapeutic cloning [2].

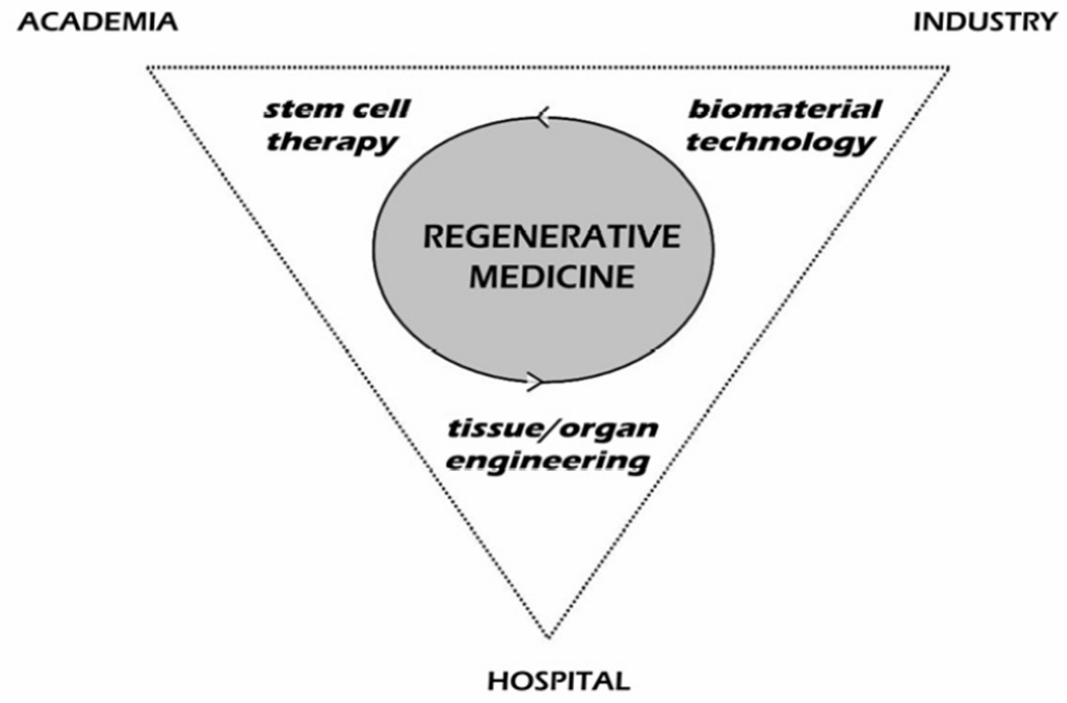

Figure 1: *The concept of regenerative medicine [3]*

The main pillars of regenerative medicine are tissue engineering, biomaterials and stem cell therapy [Figure 1].

The first pillar, tissue engineering is an interdisciplinary field that applies the principles of engineering and the life sciences for the development of biological substitutes that restore, maintain, or improve tissue function [4].

Tissue engineering is one of the most progressively developing disciplines [4-6].

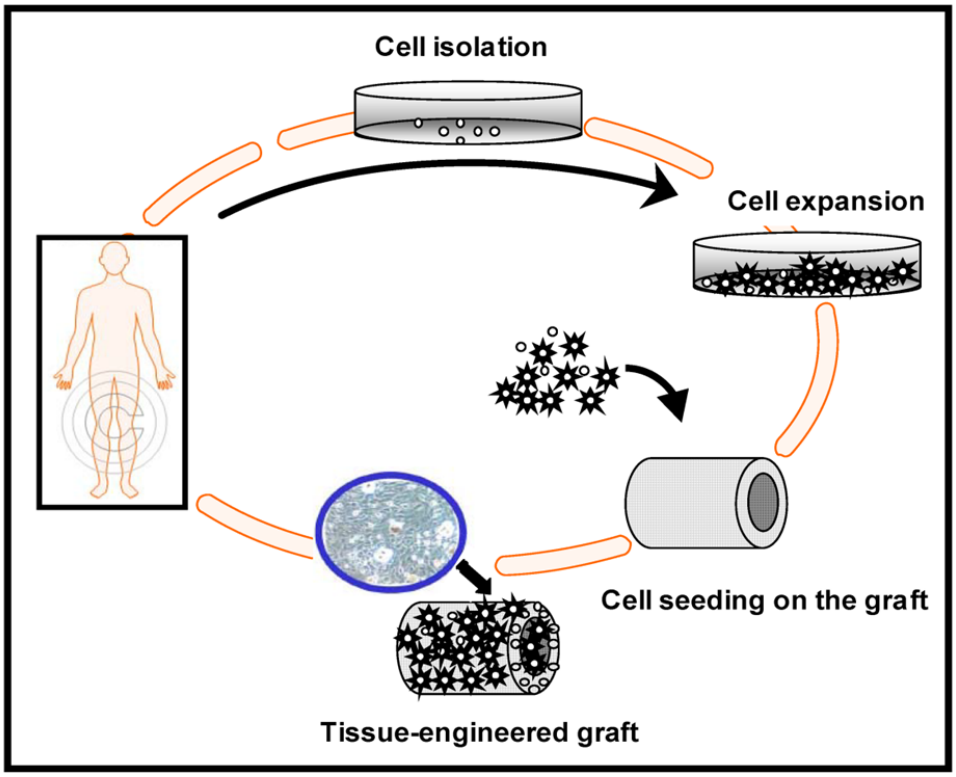

Figure 2: *The basic elements of TE [7]*

A TE process involves i) well-designed and functional microenvironments called scaffolds ii) cell culture, and iii) highly skilled implantation surgery [Figure 2]. These presuppose the cooperation of several fields of science, such as physics, materials science, chemistry, biology, genetics and the medical sciences, especially immunology. This shows that TE is not a homogenous field of science, but a highly interdisciplinary one, where all disciplines have their well-defined role.

In the early days of regenerative medicine, the application of living tissue was the primary means of recovering the damaged area. This is grafting, a technique still used in the clinical practice. While the term grafting brings first of all skin grafts to mind, virtually any kind of tissue can be grafted, depending on the aim of the intervention. The classification of grafts dates back to the early days of regenerative medicine. *Autografting* is when the source of the graft is the patient himself. This is preferred over other methods, as the risk of adverse immunological reaction is low. Autografting is still the gold standard for bone grafting [8]. With the progress of immunology, other grafts became possible. *Allografts* are taken from a genetically different member of the same species, while *xenografts* are taken from a member of a different species than the recipient. Bovine bone mineral (BBM) and porous hydroxyapatite (HA) are commonly used for xenografting [9].

Grafts, however, come with a lot of difficulties for the patients. With autografts, the donor site morbidity can cause minor complications and the surgical load of the patients is higher [10]. Transplants have high chance of rejection due to immunological reactions [11]. Xenografting has major limitations, including blood antigen incompatibility, immune responses and infectious complications [12].

The development of biomaterials opened up the way toward TE, offering an alternative to graft-based tissue regeneration.

The first, 1976 Consensus Conference of the European Society for Biomaterials defined biomaterial as ‘a nonviable material used in a medical device, intended to interact with biological systems’. In contrast, the current definition goes: ‘a material intended to interface with biological systems to evaluate, treat, augment or replace any tissue, organ or function of the body’ [13].

The two definitions demonstrate how biomaterials have moved from merely interacting with the body to influencing biological processes.

***Table 1**.: Uses of biomaterials [14]*

Problem area	Examples
Replacement of disease or damaged part	Artificial hip joint, kidney dialysis machine
Assist in healing	Sutures, bone plates and screws
Improve function	Cardiac pacemaker, intraocular lens
Correct functional abnormality	Dental implant
Correct cosmetic problem	Mammoplasty, cosmetic dentistry
Aid to diagnosis	Probes and catheters
Aid to treatment	Catheters, drains

As Table 1. describes the biomaterials can be used for various purposes. From lifesaving medical treatments, through functional regenerative surgeries to the tissue management for esthetic improvement, they are used in all aspects of medicine.

***Table 2**.: Biomaterials in organs [14]*

Organ	Example
Heart	Cardiac pacemaker, artificial heart valve, blood vessels
Lung	Oxygenator machine
Eye	Contact lens, intraocular lens
Mouth	Dental implants, fillings, crowns
Ear	Artificial stapes, cochlea implant
Bone	Bone plate, intramedullary rod
Kidney	Kidney dialysis machine Catheters, stent
Bladder	Catheters, stent

As Table 2. describes in which organs we can use biomaterials. They can be used head-to-toe in the human body. All major specialties are using them on daily basis.

Also, biomaterials can be classified by their substance.

Metals: The use of metals as biomaterials has been reported since as early as the late 18th century when iron, gold, silver and platinum were used to fabricate wires and pins to fix bone fractures [15]. It is also known that gold was used in ancient Egypt in dentistry [16]. Metals have high impact strength, high wear resistance, high ductility and the capacity to absorb high strain energy (toughness) compared to other materials. These properties make metals suitable for high-load orthopedic applications, as well as dental implants, pacer and suture wires, and coronary stents [17].

Ceramics as biomaterials are used as filling materials or covering for dental implants. Ceramics have poor fracture toughness, which limits their capability of being used in situations where load bearing is crucial. Their mechanical stiffness (Young's modulus) is high, their elasticity is low, and their surface is hard and brittle. As their chemical and structural characteristics are very similar to the mineral phase of native bone, their biocompatibility with bone is excellent. A wide range of ceramics is used in orthopedic surgery (to fill bone defects), and they are also used for the covering of implant surfaces so as to enhance osseointegration [13].

Composite biomaterials: Composites are biomaterials which have distinct phases separated on a larger-than-atomic scale, and whose characteristic properties (such as their elastic modulus) significantly differ from those of a homogenous material. In medical applications, they are most often: (1) dental filling composites, (2) reinforced methyl methacrylate bone cement and ultra-high-molecular-weight polyethylene, and (3) orthopedic implants with porous surfaces. As the constituents absorb moisture, composites have a tendency to swell. In a dental setting, this is useful, as it offsets polymerization shrinkage [14].

Polymeric biomaterials: Synthetic polymeric materials are widely used in medicine, dentistry and the pharmaceutical industry. The main advantages of these biomaterials over metal or ceramic materials include malleability, good secondary processability, reasonable cost, and availability with customized mechanical and physical properties. The desirable properties of any polymeric biomaterial are similar to those of other biomaterials: biocompatibility, resilience to sterilization, adequate mechanical and physical properties, and manufacturability [14].

Biodegradable polymeric biomaterials: These materials are broken down spontaneously via enzymatic and non-enzymatic mechanisms. Therefore, they are considered to be environmentally friendly, among their other favorable characteristics. During the past decade, we have witnessed a dramatic increase of interest in these materials. There are two main reasons for this: First, by definition, they do not elicit permanent chronic foreign-body reactions. Second, some of them have recently been found to be promising in the field of tissue engineering, especially for the fabrication of scaffolds [14]. To be suitable for such purposes, any biomaterial must meet a number of criteria. These are:

(i) Biocompatibility is essential. It is only when a material is biocompatible that the cells can migrate onto and inside the scaffold and function normally. After implantation, a biocompatible foreign body must not elicit any immune reaction so that no rejection occurs.

(ii) Biodegradability lies at the heart of the concept of implanted scaffolds. Over time, cells must be able to completely replace the temporarily implanted scaffold. The by-products of degradation should be biologically inert and able to exit the body in natural ways.

(iii) Mechanical properties: the scaffold should have mechanical properties consistent with the receptive site and it must also be resilient enough to endure surgical handling during the implantation. Producing scaffolds with proper mechanical properties is one of the current challenges in bone and cartilage engineering. The challenge here is that these scaffolds must have sufficient mechanical integrity to function from the time of implantation through the completion of the healing process.

(iv) Scaffold architecture is not less important. An interconnected pore structure and high porosity are basic requirements so that cellular penetration and adequate diffusion of nutrients to the cells are ensured. The interconnected structure also allows the diffusion of waste products out of the scaffold. As for the pores, they need to be large enough to allow cell migration into the scaffold, where they bind to their ligands. However, they must not exceed a certain size, so that a sufficient amount of specific surface remains available.

Regarding the manufacturing process, it should be rapid, reliable, and inexpensive. Another key factor is determining how a product will be delivered and made available. Clinicians typically prefer off-the shelf availability without the requirement for extra surgical

procedures in order to harvest cells prior to a number of weeks of *in vitro* culture before implantation [13].

The third pillar of regenerative medicine is stem cell therapy. Stem cells have the ability to renew themselves and differentiate into cells of any tissue (pluripotency). One option is the use of embryonic stem cells, but this raises ethical issues and the difficulties of differentiation control carry the risk of teratogenicity. Mesenchymal stem cells that reside in all sorts of tissues comprise a viable alternative.

Mesenchymal stem cells harvested from the bone marrow (bone marrow mesenchymal stromal/stem cells; BMSCs) are the best-known and -characterized type of adult stem cells. However, the use of BMSCs has serious disadvantages. These include a low cell yield from the aspirates, the painful harvesting procedure, and the potential complications.

Adipose tissue-derived stromal/stem cells (ASCs) were introduced in 2001. These cells, harvested from fat after liposuction, have the plastic-adherent character and also the ability to differentiate into several cell types (including osteoblasts and myocytes, among others). In addition, the liposuction procedure is simple, easy and repeatable. The cell yield is higher as compared to bone marrow aspiration, and the procedure is less stressful for the donor [18, 19]. Both BMSCs and ASCs are plastic-adherent under standard culture conditions, with a fibroblastic, spindle-shaped appearance. A further similarity is that both cell types form colonies in culture. However, it was found that ASCs are superior in terms of their proliferative capacity and lower senescence, and they can also be kept *in vitro* for extended periods with a stable proliferation rate [20]. In addition, the osteogenic potential and proliferation of BMSCs seems to decline with age. This decline is less marked in the case of ASCs. Therefore, it was suggested that ASCs would be more suitable for TE purposes than BMSCs. Since then, the osteogenic potential of ASCs have been proven both *in vitro* and *in vivo* [6].

II. Objectives

The main objective was to establish an innovative application in the field of regenerative medicine. We aimed to investigate a novel, scalable, rapid prototyping (RP) procedure relying on stereo-lithography (STL) and UV photocurable biopolymers *in vitro* and *in vivo*.

We had the following aims:

1. To investigate the suitability of biopolymer scaffolds for cell culturing.
2. To accomplish *in vivo* transfer of 'scaffold-cell' system.
3. To investigate biodegradability and biocompatibility of the 'scaffold-cell' system.
4. To optimize the scaffold composition for stem cells.
5. To test the tissue growing in the presence of gold nanoparticles (AuNP) added to Poly(propylene-fumarate):diethylene fumarate (PPF:DEF) scaffold.
6. To perform *in vivo* transfer of 'stem-cells-on-scaffolds'.

III. Materials and Methods

III.1 Biodegradable polymer scaffolds

a) *The Mask Projection Excimer laser StereoLithography (MPExSL) system*

MPExSL is a novel RP STL method developed by the LML laboratory in IIT, Genova. The method relies on a layer-by-layer buildup process where layers are fabricated by image projection, using pulsed excimer laser radiation [21-24]. A schematic representation of the system and a photo of the actual apparatus are shown in Figure 3.

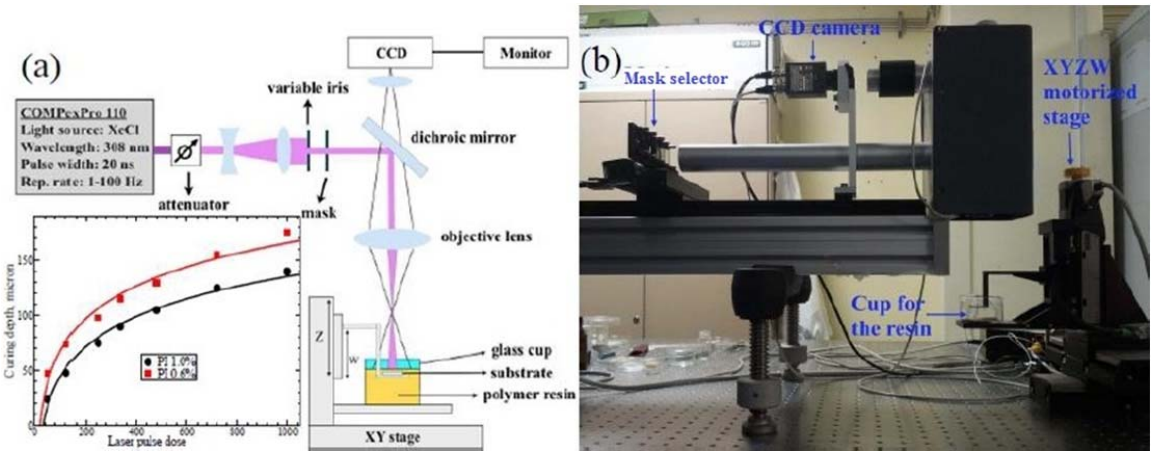

Figure 3: *MPExSL. (a) a schematic representation; (b) the actual apparatus [23]*

The output beam of a XeCl excimer laser at 308 nm is coupled to a customized mask projection optical system with a demagnification of 4, and a numerical aperture of 0.1. The system includes a telescope and a motorized variable attenuator. A motorized mask holder selects the image to be projected on the resin surface in order to form the scaffolds architecture for each layer. The mask selector, shown in Fig. 3(b) (left), consists of a precision linear stage and a holder plate that can host up to 5 masks of 25×25 mm. It is notable that in perspective the total number of masks can be increased using a compact 2-axis motorized stage or a motorized holder wheel; for example, 20 masks of 25 mm size can be loaded on a wheel of about 20 cm in diameter. With this option the scaffold architecture is the most variable. In the MPExSL technique presented hereby, lithographic photo-masks (chromium on quartz) are used, but stencil masks may also be applied. The

macro-shape of the scaffold (e.g., the scaffold diameter in the horizontal plane) can be further adjusted by means of an iris diaphragm placed right in front of the mask. The photocurable resin is in a transparent cup, supported by a multi-axis motorized stage. A charge-coupled device (CCD) camera is used to monitor the resin surface and the fabrication process on-line. Positioning of the resin surface on the lasers image plane, where the scaffold is actually built, is achieved by moving the sample with an XYZ stage. A fourth motorized stage (W) controls the vertical position of the scaffold-supporting platform immersed in the resin container cup, in order to implement the layer-by-layer fabrication. That is, after a layer is photocured, the W stage moves downwards into the resin and allows the recast of a fresh liquid resin layer on top of the previously cured layer. The applied light dose determines the depth of photocuring (layer thickness), while the magnitude of the downward step of the W stage determines the overlap between two adjacent layers. For example, to produce a layer of 120 μm thickness with a 20 μ m overlap, the following four-step procedure is necessary: i) the W stage moves downwards by 2000 μ m to immerse the cured part into the resin; ii) the W stage moves upwards by (2000-120+20) μ m; iii) a couple of minutes are left to allow the resin layer to properly recast; iv) a shot dose of light is applied to cure a 120 μ m-thick resin film. In addition, the XY stages can be moved during the fabrication procedure, increasing the flexibility of the system. During the actual fabrication process, since the W stage moves downwards, the resin surface in the cup will move upwards by a specific amount, proportional to the volume of the platform's supporting posts immersed in the resin. (This accumulating vertical shift of the resin surface is taken into account when structures with many layers are produced.) At the same time, the resin surface moves out of the preset image plane. This is also taken into account by moving the Z stage downwards, keeping the resin surface within the depth of focus of the optical system. The entire process is computerized. It is to be noted that the above procedure uses a passive recasting method. Diethyl fumarate (DEF) is applied as diluent to reduce the resin viscosity as needed for proper resin recast. When using 308 nm light and PPF:DEF (7:3 w:w) resin with 0.6 wt% or 1.0 wt% PI (BAPO, Irgacure 819), the curing depth can be very well controlled in the 20 to 170 μm range by varying the applied laser pulse dose, as shown in the inset of Fig. 3(a). In this way, the thickness of the layers building up the 3D scaffold can be well controlled, with a

micrometer resolution and avoiding over-curing, which is essential for reliable and precise scaffold fabrication. Indeed, the UV light at 308 nm is absorbed to some extent also by the PPF polymer resulting in a self-limited light penetration into the resin. When using longer wavelength light, i.e., near-UV/visible, the use of absorbers/scatterers into the resin, e.g., dyes or nanoparticles, is often necessary in order to limit the light penetration depth, control the curing depth, and avoid over-curing[23].

b) *Resin and Photoinitiators*

PPF is a versatile biodegradable and photocurable biomaterial, a linear polyester with an unsaturated backbone that allows the crosslinking, and cytocompatible degradation products based on propylene glycol and fumaric acid [25]. The PPF used in this work is not commercially available. It was synthesized for the purposes of the study. Briefly, fumaric acid was heated in excess of propylene glycol at 145°C with overhead mechanical stirrer. A Barrett trap was connected beneath the condenser to collect water, produced as a by-product. After 3 to 4 hours, the temperature was increased to 180°C for 2 hours to collect the unreacted propylene glycol, and viscosity was checked. The polymer was purified by methylene chloride, followed by water and brine. Sodium sulphate was used as a drying agent of the organic phase, and finally, the PPF was made solvent-free via a rotary evaporator [22]. To have an appropriate viscosity for STL purposes, the purified PPF resin had to be diluted. Diethyl fumarate (DEF) was applied as diluent to reduce the resin viscosity as needed for proper resin recast [21-24]. Irgacure 819 or Bis(2,4,6-trimethylbenzoyl)-phenylphosphineoxide „BaPO" [26] is used with the PPF:DEF due to its favorable spectrum in the deep UV, as well as being ethanol-soluble, thus compatible with the resin mixing process.

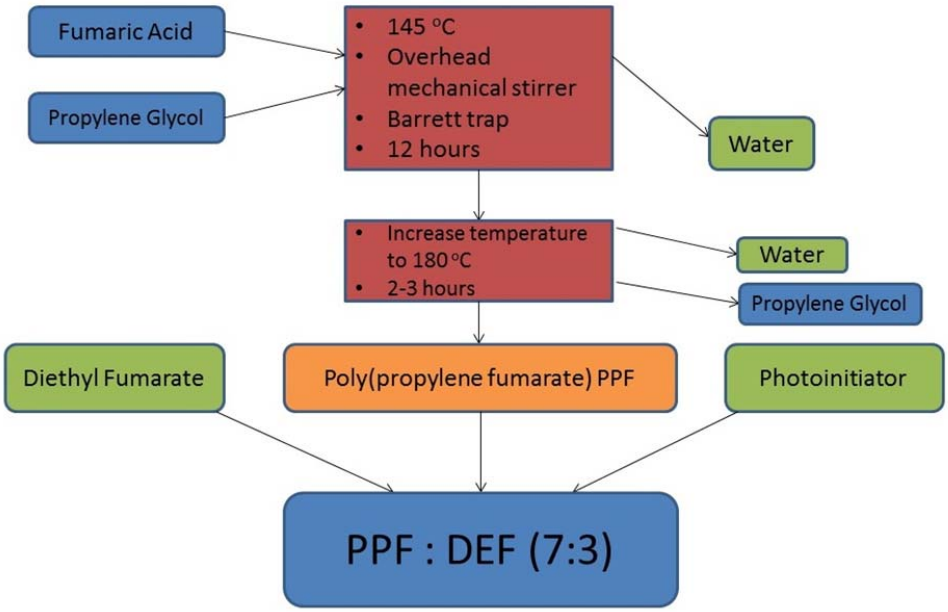

Figure 4: *PPF:DEF synthesis [22]*

c) *NP integration to the resin:*

The particle of choice was gold nanoparticles. AuNPs are ideal platforms for drug/growth factor delivery as well as Deoxyribonucleic acid (DNA) adhesion, and they are also easy to produce. All chemicals were commercially available and used unless otherwise stated. The Au NPs (with a diameter of 13 ± 1 nm, 85 %) were prepared by a standard citrate reduction protocol. A solution of hydrogen tetrachloroaurate trihydrates ($HAuCl_4.3H_2O$, Alfa Aesar 99.9% (metal base) Au 49% min) 1 mM was boiled, then 3 ml of 30 mM trisodium citrate (Sigma Aldrich, USA) aqueous solution was injected under vigorous stirring for 20 min. When the solution cooled down, the nanoparticles were separated by centrifugation. After each centrifugation cycles, the supernatant was replaced with Milli-Q water of 18.2 MΩ resistance, resulting in NPs dispersion in water. The particles' concentration, optical absorption, and size were determined by inductively coupled plasma optical emission spectrometry (ICP-OES), spectrophotometry, and electron microscope, respectively. In order to increase the dispersion of Au NPs inside the resin, 90 mg of Polyvinylpyrrolidone (PVP) (Sigma Aldrich, MW 10 KDa) was added to the water dispersion. The final concentration of PVP was adjusted to be 3 mg/ml. The reaction solution was stirred overnight. Finally, the coated nanoparticles were collected and cleaned from excess PVP by

three cycles of centrifugation with the supernatant exchanged with Milli-Q water (18.2 MΩ) each time. The coating process was repeated twice. In the end, the coated NPs were dispersed in ethanol prior to any further processing. The NPs only exhibited excellent colloidal stability in ethanol after these two cycles of PVP coating (PVP I and PVP II, respectively). The PVP-coated nanoparticles retained their dispersion stability in the organic DEF medium as well. Both dispersion of PVP-coated NPs (Au NP/PVP) in the DEF and the PPF:DEF matrices optical absorption was investigated. This ethanol colloidal of PVP-coated Au NPs was then mixed to DEF (Aldrich) by means of sonication (30 min) and stirring (24 hours). With the identified particle size, the final concentration of the Au NPs in the DEF was detected to be 18.4 μM by means of ICP-OES. Using the NP-embedded DEF, a series of PPF:DEF-Au NP nanocomposite resins were prepared for MPExSL: first the DEF-Au NP was mixed with pristine DEF and stirred for 1 hour, then added to the PPF. The photoinitiator was added to this reaction mixture [27]

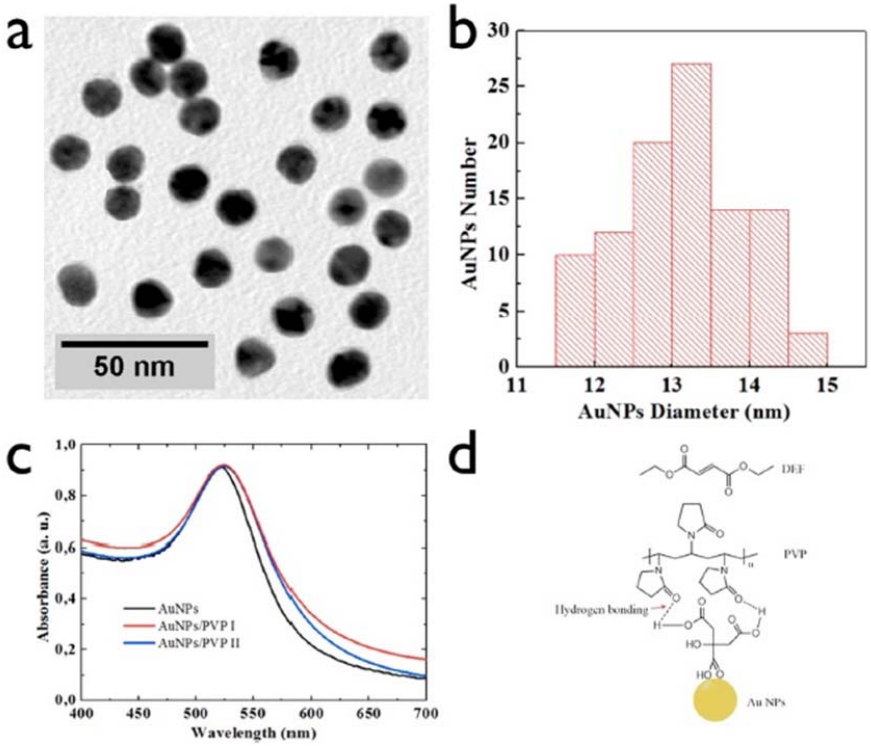

Figure 5: *(a) TEM micrographs of Au NPs in aqueous dispersion capped with TSC, (b) histogram of the nanoparticle size distribution. (c) Optical absorption spectra of Au NPs in aqueous dispersion and after two cycles of PVP coating in ethanol medium. (d) Scheme illustrated the possible bonding of citrate molecule capped Au NPs with PVP coating and diethyl fumarate molecules [27]*

III.2 Biological testing

III.2.1. Tested scaffold types

For the *in vivo* and *in vitro* tests, 5 mm diameter, 100 μm thick porous scaffolds were prepared with 200 μm-pore diameters, using a BaPO concentration of 1%. Two types of these, PPF:DEF scaffolds with 200 μm pore size were used. The first type of scaffolds did not contain any NPs. The resin included 5.52 μMAu NPs, in the second type of scaffolds.

III.2.2. Preparation of scaffolds

The photocured samples were sterilized with UV irradiation for 30 min and coated with 0.01% poly-L-lysine (MW 70000-150000 Da, Sigma-Aldrich, USA) for 30 min at room temperature. Poly-L-lysine was removed and the scaffolds were dried under laminar box, and then incubated in Eagle's Minimum Essential Medium (EMEM, Lonza, Switzerland) with 10 % fetal bovine serum, 100 U/ml penicillin, 100 U/ml streptomycin and 0.25 μg/μl Fungizone (PromoCell GmbH, Heidelberg, Germany) for 7 days at 37 °C. The medium was changed every other day. At day seven, cells were seeded.

III.2.3. Cell types and culture condition

- *K7M2*

  K7M2 mouse osteosarcoma cell line cells (provided by Dennis Klinman, NCI-Frederick, MD, USA) were seeded 2 x 10^5 cells/ml in wells, containing one scaffold each, in EMEM, and then incubated in humidified atmosphere with 5% CO_2 at 37 °C for 14 days. K7M2 cell line was derived by intra-osseous injection of the K7 murine osteosarcoma cell line to the proximal tibia of a Balb/c mouse. The resultant primary tumor spontaneously metastasized to the lungs. A pulmonary metastasis was removed from the lung and then surgically implanted to a paraosteal tibial muscle flap of a naïve mouse. This cycle of implantation of pulmonary metastasis to paraosteal tibial muscle flap sites was repeated, resulting in the K7M2 primary tumor. This tumor was dissociated to a single cell suspension to create the K7M2 wt cell line [28].

- *RAW 264.7 Cell Line murine, macrophage from blood*

  RAW 264.7 murine cell line was obtained from Sigma-91062702. The cells were seeded at 5×10^4 cells/ml in wells containing one scaffold each, and then incubated in humidified atmosphere with 5% CO_2 at 37 °C for 4 days. RAW 264.7 cell line was established from an ascites of a tumor induced in a male mouse by intraperitoneal injection of Abselon Leukaemia Virus (A-MuLV). Cells will pinocytose neutral red and phagocytose zymosan. Cells are capable of antibody dependent lysis of sheep erythrocytes and tumor targets. [29]

- *ASC*

  Primary autologous adipose stem cells were isolated from 4 to 6 weeks old Balb/c male mice (Charles River Laboratories International, Inc.). After cervical dislocation, the abdominal adipose tissue was removed. The tissue was put in 100 µg/ml RPMI (Cat.No.: BE12- 115F, Lonza, Switzerland), treated with kanamycin (Kanamycin sulfate from Streptomyces Kanamyceticus, Sigma K 1377-16, Sigma-Aldrich, USA), then digested in collagenase (Sigma-Aldrich, USA) at 37 °C. After 1 hour, the cells were washed and cultured in a Petri dish for 2 weeks in MSC Medium (MesenCult, STEMCELL, Canada) with 10% fetal bovine serum, 100 U/ml penicillin, 100 U/ml streptomycin and 0.25 µg/µl Fungizone (PromoCell GmbH, Heidelberg, Germany) at 37 °C, 5% CO_2. These cells were seeded at 5×10^4 cells/ml in wells containing one scaffold each, and then incubated in humidified atmosphere with 5% CO_2 at 37 °C for 4 days.

III.2.4. *In vitro* experimental set-up

Cell-seeded-scaffolds with cells were prepared for scanning electron microscopic (SEM), and confocal microscopic examination. For the preparation for confocal microscopy, we used 4% paraformaldehyde and immune staining (Alpha tubulin, Phalloidin, Dapi, Tomato). SEM samples were treated with 0.1 M Sodium Cacodylate and 1.2% Glutaraldehyde. Samples were dehydrated in ethanol of increasing concentration (50%, 70%, 80%, 90%, 96%, 100%) for 10 min each concentration and 100% Hexamethyldisilazane overnight.

III.2.5 *In vivo* experimental set-up

- *K7M2*

  K7M2 mouse osteosarcoma cell line was grown on the scaffolds for 14 days before implantation in mice. After being covered with cells, the scaffolds were implanted under the dorsal skin of 8-week old female Balb/C mice (Charles River Laboratories International, Inc.). Control groups were implanted with cell-free scaffolds. 14 days after transplantation, the scaffolds and dorsal skin were removed and blood samples were collected. For the purposes of cytokine and chemokine profiling, the collected blood samples were allowed to clot for 30 min at room temperature, then overnight at 4 °C. Serum samples were collected by centrifugation at 3000 rpm for 5 min and stored at −80 °C until the time of analysis. Five mice per group were implanted. In case of a successful cell implantation, the presence or absence of selected K7M2 mouse osteosarcoma cell line was followed by histology. Animal care was provided in accordance with the procedures outlined in the protocol authorized by the Institutional and the National Animal Ethics and Experimentation Boards

- *ASC*

  After being covered with cells, the scaffolds were implanted under the dorsal skin of 8-week-old female Balb/c mice (Charles River Laboratories International, Inc.). The control group was injected with 5×10^4 cells/ml ASCs. Three mice per group were implanted. 14 days after implantation, the scaffolds and dorsal skin were

removed and blood samples were collected. For the purposes of cytokine and chemokine profiling, the collected blood samples were allowed to clot for 30 min at room temperature, then overnight at 4 °C. Serum samples were collected by centrifugation at 3000 rpm for 5 min and stored at −80 °C until the time of analysis. In case of a successful cell implantation, the presence or absence of selected mouse ASC was followed by histology. All animal experiments were performed in accordance with national (1998. XXVIII; 40/2013) and European (2010/63/EU) animal ethics guidelines. The experimental protocols were approved by the Animal Experimentation and Ethics Committee of the Biological Research Centre of the Hungarian Academy of Sciences and the Hungarian National Animal Experimentation and Ethics Board (clearance number: XVI./ 03521/2011.).

III.2.5.1. Cytokine and chemokine proteome profiler

The potential inflammatory reactions of the implanted biomaterial were screened via cytokine and chemokine profiling. Protein concentrations of the sera were measured by BCA Protein Assay (Thermo Scientific, USA) and pooled samples were tested to simultaneously detect relative levels of different cytokines according to the manufacturer's instruction by Mouse Cytokine Array, Panel A (R&D Systems, USA). Immunoreactive signals were detected using a LI-COR ODYSSEY® Fc (Dual-mode imaging system) imager followed by analysis with Odyssey v1.2 software.

III.2.5.2. Histology

Specimens were fixed in 4% buffered paraformaldehyde and then embedded into paraffin blocks. Four-micrometer-thick sections were prepared and stained by conventional hematoxylin-eosin stain then cover-slipped. The sections were visualized by scanning virtual microscope (3D Histech, Hungary).

III.2.5.3 FISH

Fluorescence in situ hybridization (FISH) is a molecular diagnostic technique utilizing labeled DNA probes to detect a gene or specialized sequences. The sample DNA (metaphase chromosomes or interphase nuclei) is first denatured, a fluorescently labeled probe of interest is then added to the denatured sample and hybridizes with the sample DNA at the target site as it re-anneals back into a double stranded DNA. The probe signal can then be seen through a fluorescent microscope and the sample DNA can be scored for the presence or absence of the signal [30]. For fluorescence in situ hybridization (FISH), chromosome X and Y control probe (Empire Genomics, Buffalo, NY, USA) was used, to verify the presence of the Y chromosome of the transplanted mouse adipose stem cells, according to the manufacturer's instructions.

IV. Results

1. K7M2 cells were successfully seeded to biopolymer scaffold.

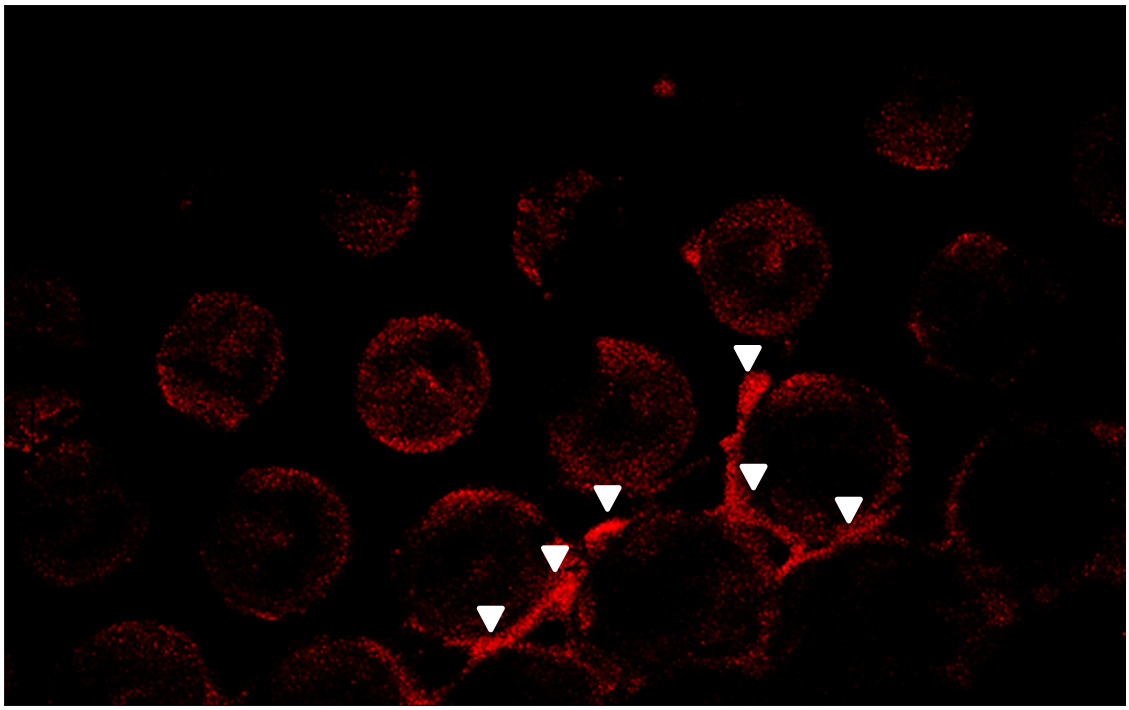

Figure 6*: Stained K7M2 cells can be seen on the fluorescent microscopic image of the scaffolds, around the pores.*

After 14 days of incubation, fluorescent microscopic images were taken of the scaffold, with Tomato red transfected cells as seen in *Figure 6*. Viable red cells adhered to the margin of pores (indicated by arrowheads).

2. K7M2 seeded scaffold successfully transferred cells *in vivo* and did not induce immune rejection

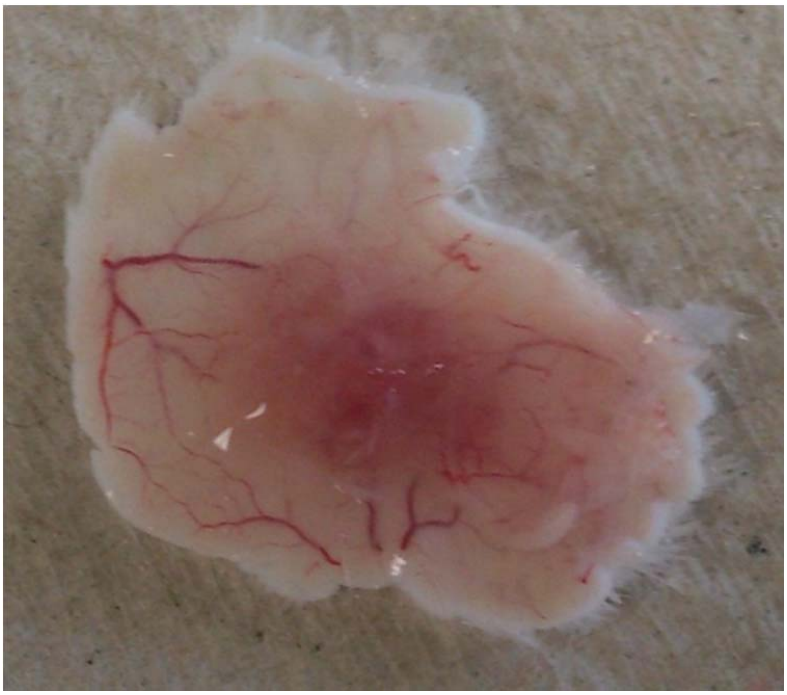

Figure 7*: The removed dorsal skin area, no visible sign of inflammation*

14 days after implantation, the implantation site, the dorsal skin of the mice were removed (Fig. 7.), and blood samples were collected. A small size nodule was visible in each mouse implanted with K7M2 seeded scaffold, but we could not observe wound, inflammation, bleeding or ulceration. The experimental animal did not show high temperature, pain, scratching, any symptom or side effect.

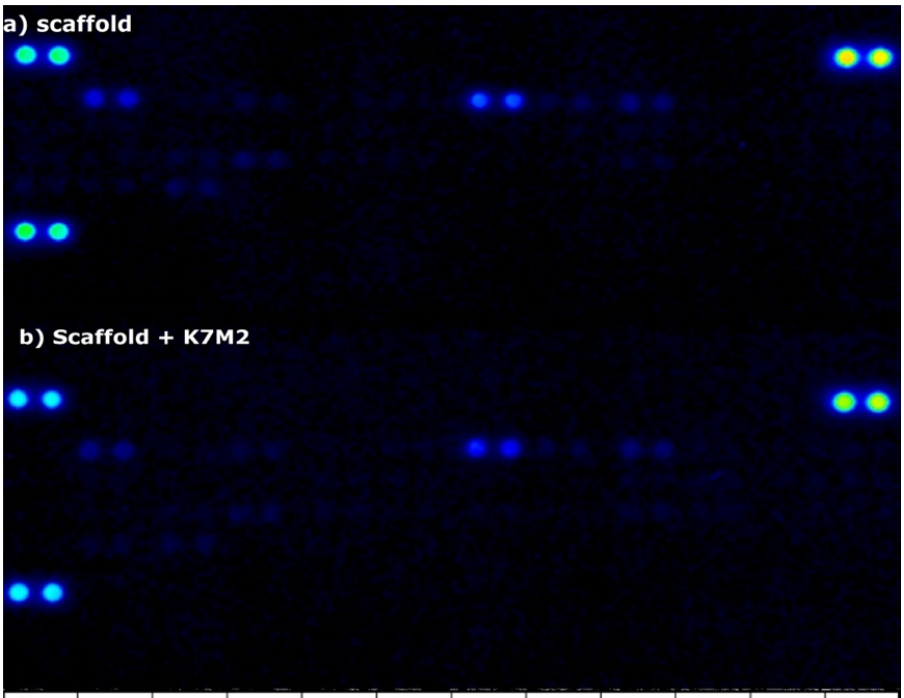

Assay contr.											Assay contr.
CXCL 13	C5a	G-CSF	GM-CSF	CCL-1	CCL11	CD54	IFN-γ	IL-1α	IL-18	IL1-RA	IL-2
IL-3	IL-4	IL-5	IL-6	IL-7	IL-10	IL-13	IL12 P70	IL-16	IL-17	IL-23	IL-27
CXCL10	CXCL11	IL-8	M-CSF	CCL2	CCL-12	CXCL9	CCL3	CCL4	MIP-2	CCL5	CXCL12
CCL 17	TIMP-1	TNF-α	TREM-1								
Assay contr.											

Figure 8: *Cytokine and chemokine profile of (a) control sera and (b) tumor scaffold-implanted mice sera. The spreadsheet shows the cytokine and chemokine map.*

The collected blood samples were cytokine and chemokine profiled. No significant difference was detected between the cytokine profiles of the tumor scaffold- implanted group and the control group (Fig 8). We could not find elevated level of proinflammatory cytokines or chemokines.

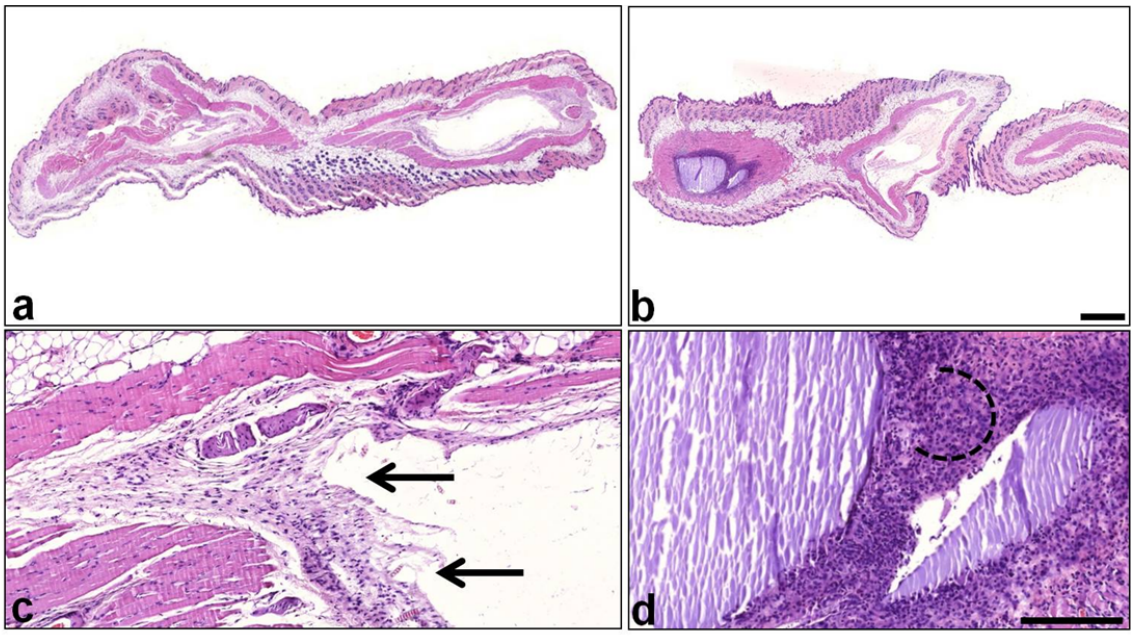

Figure 9: *Images of the control scaffold (a) and the K7M2 tumor cell seeded scaffold (b) implanted sections. Only a mild fibrotic reaction was observed around the control scaffold (c-arrows), whereas viable foci of anaplastic sarcomatous tumor cells embedded in dens inflammatory reaction were seen in the tumor scaffold specimen (d, dashed line indicates tumor border). /HE; OM 200x; a-b and c-d scale bar 1000um and 200um, respectively/*

Upon histological examination of the implanted scaffolds, no signs of inflammation were observed in the dorsal skin, and no signs of rejection were found. In the histological sections of the group implanted with tumor cell seeded scaffolds (Fig. 9 b and d), viable, anaplastic sarcomatous tumor cells were found. In Fig 9 d, the dashed line indicates tumor border. In contrast, in the control mice only a mild fibrotic reaction was observed around the location of the scaffold (Fig 9c, arrows). No residual biopolymer piece was found at the transplantation site in the control animals, suggesting the biological degradation of the scaffolds.

3. AuNP filled scaffolds support stem cell adherence and viability compared to AuNP free material

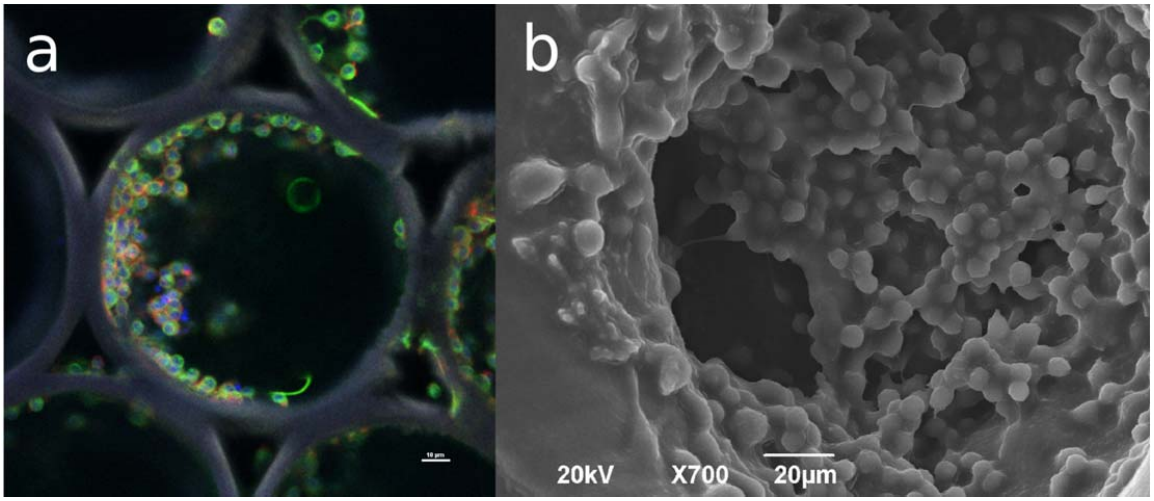

Figure 10: *Scaffold of 200 µm pore size, with Au nanoparticles and macrophages a) confocal microscopy, b) SEM*

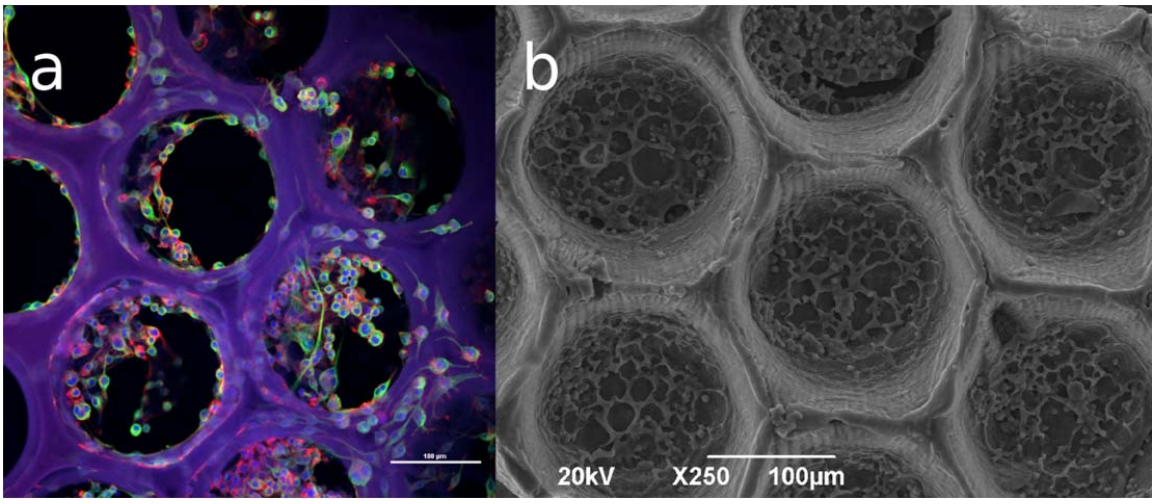

Figure 11: *Scaffold of 200 µm pore size, without Au nanoparticles and with macrophages a) confocal microscopy, b) SEM.*

In vitro, macrophages - a cell type of high adherence - could be seeded on the scaffold surface as shown in Fig. 10. The Au-content of the polymer resin had no influence on the adherence of the macrophages (Fig. 11).

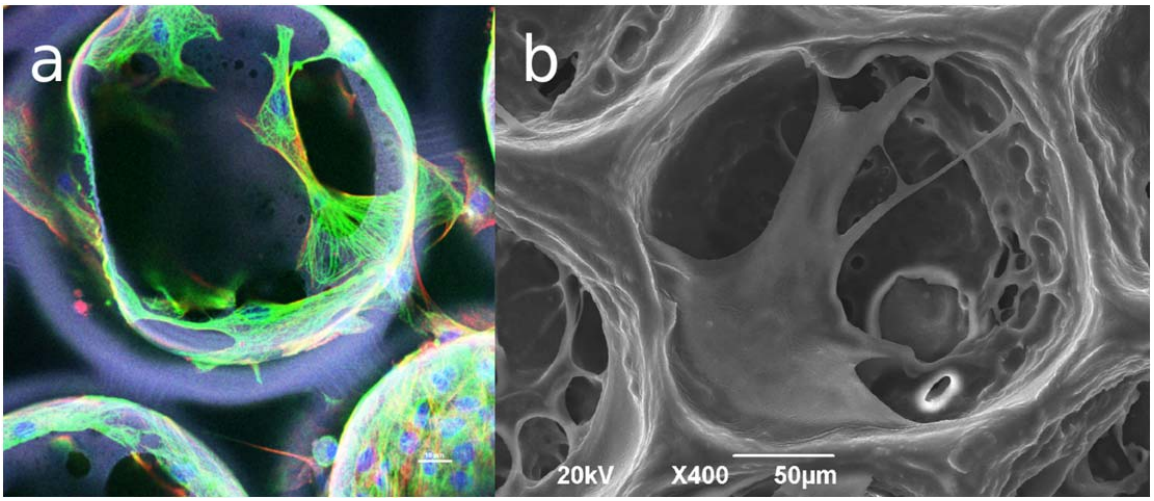

Figure 12: *Scaffold of 200 µm pore size, with Au nanoparticles and with mouse ASCs a) confocal microscopy, b) SEM.*

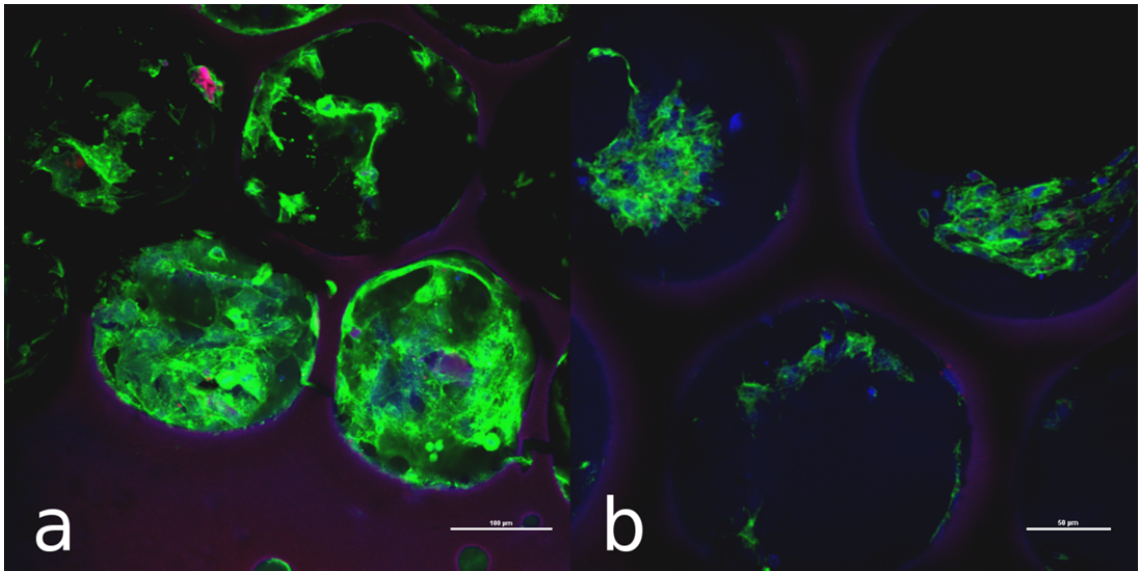

Figure 13: *ASC adhesion to a hybrid (a) and a normal (b) scaffold*

The adherence of ASCs, however, was apparently affected by the Au content of the scaffold. Adherence to the Au NP hybrid scaffold proved to be much better (Figs. 12, 13). Stem cells adhered to the surface of AuNP filled scaffolds. ASCs did not show appropriate proliferation on the surface of the AuNP-free scaffolds, cell aggregates were seen in the middle of pores (Fig. 13b).

4. Stem cell seeded scaffold induced muscle regeneration in vivo

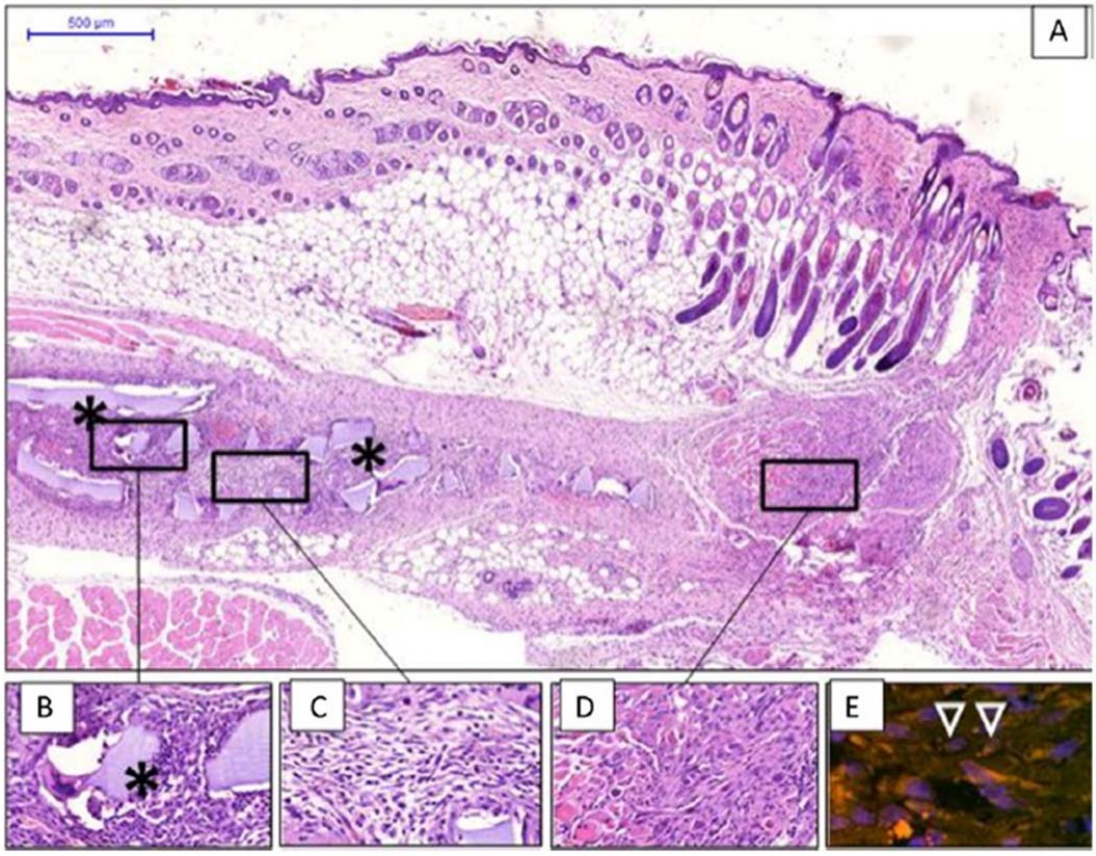

Figure 14*: Images of a section with ASC- seeded Au- filled scaffold (A, B, C). Viable mesenchymal cell colonies and striated muscle regeneration indicated by stem cells were seen in the scaffold (D). The Y chromosome content of the transplanted stem cells was detected by FISH, indicated by arrowheads (E).*

The excised skin areas showed no visible signs of reactive inflammation (Fig. 14), and the cytokine profiling did not indicate inflammation either (Fig. 15). Interestingly, we detected not only the implanted ASCs with X-Y chromosome but also cells containing Y and more than one X chromosomes (data not shown), most likely resulting from regenerative cellular fusion between ASCs and stromal mesenchymal cells (Fig. 14A). This suggests that the biopolymers applied together with ASCs were able to initiate tissue repair in the appropriate tissue environment. In the histological sections of the group implanted with ASCs, small residual biopolymer pieces of varying diameter (50– 500 μm) were seen.

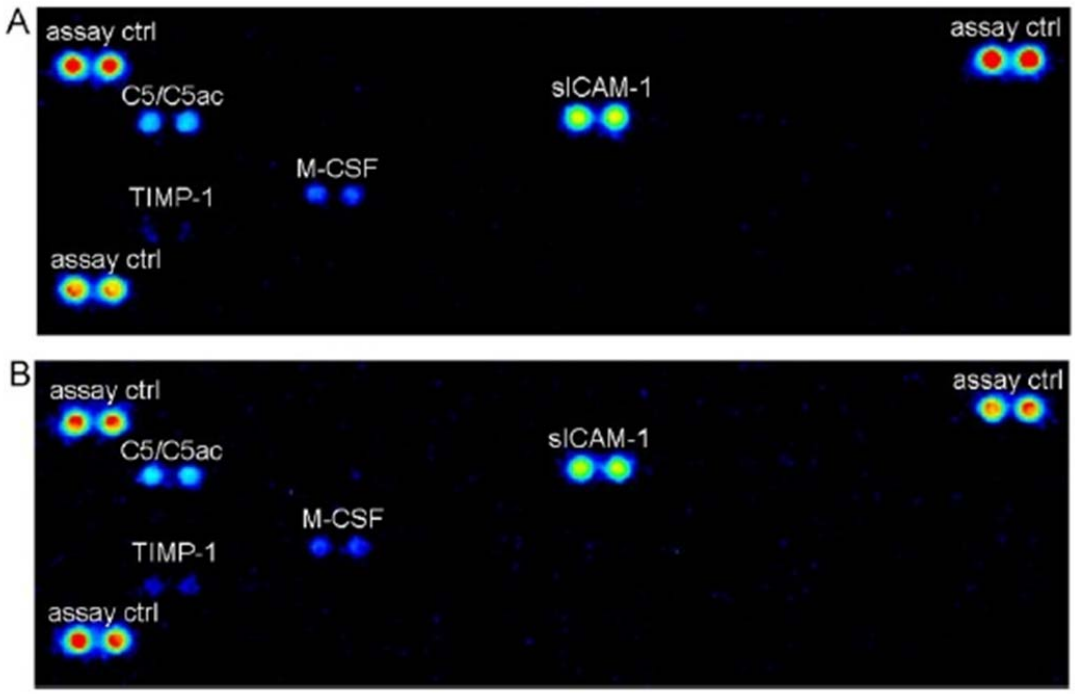

Figure 15: *Results of the in vivo cytokine profiling:*
The cytokine and chemokine profiling detected C5, sICAM-1, M-CSF and TIMP-1. The profiler did not indicate significant immune reaction to the ASC-seeded scaffolds (A) as compared to the control scaffold (B). This is supported by the lack of immune cell infiltration or relevant immune reaction against the ASC-seeded scaffold, as revealed by histology.

V. Discussion

The main objective we set was to test a novel, scalable, rapid prototyping (RP) procedure relying on stereo-lithography (STL) and UV photocurable biopolymers *in vitro* and *in vivo*.

The first experiment was built around the fundamental questions of scaffold use. We investigated cell adhesion, biocompatibility and biodegradability [31]. Tissue engineering scaffolds are usually made of polyester. Three types are used most frequently [32]: (i) Polycaprolacton (PCL) is used in various forms, such as films, fibers, and microparticles [33-35]. To improve its bioactive properties, it is used in the form of composite materials with other polymers, such as gelatin and chitosan, in various tissue regeneration contexts [36, 37]. (ii) Poly (L-lactic acid) (PLLA) is a synthetic biodegradable polyester formed through the polymerization of l-lactide, obtained from renewable sources such as starch. It has a wide variety of applications including sutures, drug delivery vehicles, prosthetic devices, vascular grafts, bone screws, skin regeneration scaffolds, and pins for fixation [38]. (iii) Poly(lactic-co-glycolic) acid (PLGA) is a combination of the polyester polymers PLLA and poly(glycolic acid) (PGA) and is among the most commonly used biodegradable synthetic polymers for tissue engineering applications [39]. Our scaffold material, PPF:DEF is a relatively new material [40]. However for bone TE applications the photocross-linking of poly(propylene fumarate) (PPF) was investigated to form porous scaffolds [41]. For the formation of cross-linked, degradable polymer networks with tunable material properties cross-linking factors have been examined in combination with PPF [42], but this precise combination was first described by Kasper and colleagues in 2009 [25] and it needed further investigation.

In our study, we covered PPF:DEF scaffolds with K7M2 mouse osteosarcoma cells, and we were able to transfer this ‘scaffold-cell’ system into the living tissue, i.e. into recipient mice. No signs of inflammation were detected, either by the cytokine/chemokine profiling or with histology. No scaffold remnants were found in the histological sections, which indicate that the scaffold was biologically degraded. In this sense, we can say that our system met the three fundamental requirements towards scaffolds: adhesion, mechanical strength, and biocompatibility/biodegradability [31].

After having proven that the scaffolds were fit for tissue engineering, we took a step forward: we wished to optimize the system to stem cells, because regenerative medicine is based on the trinity of stem cells, biomaterials and tissue engineering [3] and all medical fields investigate stem cell driven regeneration [32, 43].

Our results showed that the stem cells are sensitive to the composition of the scaffolds. We performed *in vitro* experiments with scaffolds of different concentration of incorporated AuNPs. While the stable but transformed macrophage cell line was not especially sensitive to the Au-content of the polymer, the adherence and distribution of ASCs was definitely better on the Au hybrid polymer. This is important because of the potential value of these cells in regenerative tissue engineering. The incorporated AuNPs helped the stem cells adhere to the scaffolds. The results of the *in vivo* experiment showed that our cell-scaffold complex could be successfully transferred into the living tissue of experimental animals and the stem cells induced muscle regeneration.

Tumor formation is an ever-present danger of stem cell transplantation, but our system proved to be safe in this respect. The use of the scaffold ensures that the cells are kept in place, and the chance of stem cells getting into the bloodstream is significantly reduced. The use of autologous stem cells reduces the risk of rejection, ensures better regeneration, and ASCs are readily available. ASCs are easy to harvest in a safe, minimally invasive way from almost any patient

Our research about PPF:DEF scaffolds are pointing in the future. The results show that this scaffold is an adequate option in regenerative medicine. It needs further research until it gets to the clinical use, but the first steps were made.

Summary of accomplished objectives:

- We have proven, the PPF:DEF biopolymers scaffolds are suitable host for cell cultures
- We are able to transfer 'scaffold-cell' system in living experimental animals
- The scaffolds are biocompatible and biodegradable TE devices
- Incorporated NPs (especially au NPs) in the scaffold composition can enhance tissue growing
- We are able to manage autogenous adipose tissue-derived stem cells to PPF:DEF scaffolds and transfer, this complex in experimental mice.

VI. Conclusion

The studies described in this thesis were planned to take the PPF:DEF scaffolds closer to the clinical application.

In vitro and *in vivo* experiments were conducted to prove that the scaffolds meet the *sine qua non* requirements of medical use. When it was established, we turned our attention to application with stem cells.

The PPF:DEF scaffold proved to be a competent tissue engineering device, because it was biocompatible, biodegradable, and cells could adhere to it, and it's meeting the expectations when it gets to the application. Furthermore, the adipose stem cells could be transported with the scaffold to experimental animals. We also noticed that AuNPs supplementation of the scaffold enhanced cell adhesion and proliferation.

The future of this research should be continued towards the clinical usage. We did the first steps, and after the basics, it should carry on, because the scaffold is promising. Further experiments need to show, that the scaffolds can be used in bigger size, with more cells, to cover up a bigger surface. It is necessary to work out more precise experiments *in vivo* towards regenerative medicine. A standardized method could facilitate the hard and soft tissue regeneration, renewing thereby restorative, regenerative medicine.

VII. Acknowledgments

First of all, I wish to thank my **co-supervisor, Professor Katalin Nagy**, Former Dean of the Faculty of Dentistry, Head of Oral Surgery Department for her constant help, support and supervision. Throughout the years, she has supported me in all my goals developing professionally. Without her guidance I wouldn't be anywhere near the research side of dentistry.

Also I would like to thank my **co-supervisor, Krisztina Buzás, Ph.D.**, for her patience towards me. She was the one who have shown me, that basic research can be fun and with her help I was able to broaden my mind and travel the world.

Special thanks **Szabolcs Beke, Ph.D**. He became more than a colleague through the years, he became a friend. Show me that physics is more what I imagine, and help me getting used to live abroad.

I would like to thank the research team **Edina Gyukity-Sebestyén, Mária Harmati, Gabriella Dobra**. They taught me all the lab skills, without them the cells wouldn't live for more than 24 hours.

I'm also grateful to **Kinga Turzó, Ph.D.,** Dean of Faculty of Dentistry, **Professor János Minárovits** they showed me a way into the fantastic world of research.

I thank **István Németh, Ph.D.** for his cooperation in the histological investigations.

And also thank to **Gábor Braunitzer, Ph.D**. who showed me the stylish way of publishing.

Last but not least I would like to thank to my family, my friends who gave me inspiration and endurance for the whole project.

And my biggest support, my fiancée **Zsófia Tarnai**, with whom I met during the PhD program, we were the whole class and doing reunions on daily basis.

VIII. References:

1. *https://report.nih.gov/nihfactsheets/ViewFactSheet.aspx?csid=62.*
2. Kemp, P., *History of regenerative medicine: looking backwards to move forwards.* 2006.
3. Andrades, J.A., et al., *Skeletal Regeneration by Mesenchymal Stem Cells: What Else?* 2011: INTECH Open Access Publisher.
4. R. Langer, J.P.V., *Tissue Engineering.* Science, 1993. **260**: p. 920.
5. Trumbull, A., G. Subramanian, and E. Yildirim-Ayan, *Mechanoresponsive musculoskeletal tissue differentiation of adipose-derived stem cells.* Biomed Eng Online, 2016. **15**: p. 43.
6. Liao, H.T. and C.T. Chen, *Osteogenic potential: Comparison between bone marrow and adipose-derived mesenchymal stem cells.* World J Stem Cells, 2014. **6**(3): p. 288-95.
7. Alvarez, K. and H. Nakajima, *Metallic scaffolds for bone regeneration.* Materials, 2009. **2**(3): p. 790-832.
8. Rogers, G.F. and A.K. Greene, *Autogenous bone graft: basic science and clinical implications.* J Craniofac Surg, 2012. **23**(1): p. 323-7.
9. Browaeys, H., *A Literature Review on Biomaterials in Sinus Augmentation Procedures.* Clinical Implant Dentistry and Related Research, 2007. **9**(3): p. 166-177.
10. Banwart, J.C., M.A. Asher, and R.S. Hassanein, *Iliac Crest Bone Graft Harvest Donor Site Morbidity: A Statistical Evaluation.* Spine, 1995. **20**(9): p. 1055-1060.
11. Immunity after organ transplantation, Jean Villard, Swiss Med Wkly, 2006
12. Ekser, B., et al., *Clinical xenotransplantation: the next medical revolution?* The Lancet, 2012. **379**(9816): p. 672-683.
13. O'Brien, F.J., *Biomaterials & scaffolds for tissue engineering.* Materials Today, 2011. **14**(3): p. 88-95.
14. Patitapabana Parida, A.B., Subash Chandra Mishra, *Classification of Biomaterials used in Medicine.* International Journal of Advances in Applied Sciences, 2012. **1**(3): p. 31-35.
15. Bhat, S. and A. Kumar, *Biomaterials and bioengineering tomorrow's healthcare.* Biomatter, 2013. **3**(3).
16. Donaldson, J., *The use of gold in dentistry.* Gold bulletin, 1980. **13**(3): p. 117-124.
17. Moravej, M. and D. Mantovani, *Biodegradable metals for cardiovascular stent application: interests and new opportunities.* Int J Mol Sci, 2011. **12**(7): p. 4250-70.
18. Zuk, P.A., et al., *Multilineage cells from human adipose tissue: implications for cell-based therapies.* Tissue Eng, 2001. **7**(2): p. 211-28.
19. Duscher, D., et al., *Ultrasound-assisted liposuction provides a source for functional adipose-derived stromal cells.* Cytotherapy, 2017.
20. Kern, S., et al., *Comparative analysis of mesenchymal stem cells from bone marrow, umbilical cord blood, or adipose tissue.* Stem Cells, 2006. **24**(5): p. 1294-301.

21. Beke, S., et al., *Towards excimer-laser-based stereolithography: a rapid process to fabricate rigid biodegradable photopolymer scaffolds.* J R Soc Interface, 2012. **9**(76): p. 3017-26.
22. Beke, S., et al., *Rapid fabrication of rigid biodegradable scaffolds by excimer laser mask projection technique: a comparison between 248 and 308 nm.* Laser Physics, 2013. **23**(3): p. 035602.
23. Beke, S., et al., *3D scaffold fabrication by mask projection excimer laser stereolithography.* Optical Materials Express, 2014. **4**(10): p. 2032.
24. Farkas, B., et al., *Four-order stiffness variation of laser-fabricated photopolymer biodegradable scaffolds by laser parameter modulation.* Mater Sci Eng C Mater Biol Appl, 2015. **55**: p. 14-21.
25. Kasper, F.K., et al., *Synthesis of poly(propylene fumarate).* Nat Protoc, 2009. **4**(4): p. 518-25.
26. Datasheet of Irgacure 819 (Sigma Aldrich)
27. Abdelrasoul, G.N., et al., *Nanocomposite scaffold fabrication by incorporating gold nanoparticles into biodegradable polymer matrix: Synthesis, characterization, and photothermal effect.* Mater Sci Eng C Mater Biol Appl, 2015. **56**: p. 305-10.
28. Khanna, C., et al., *An orthotopic model of murine osteosarcoma with clonally related variants differing in pulmonary metastatic potential.* Clinical & experimental metastasis, 2000. **18**(3): p. 261-271.
29. RAW 264.7 (ECACC 91062702) cell line datasheet from European Collection of Authenticated Cell Cultures
30. https://www.empiregenomics.com/store/fish_probes
31. Holzwarth, J.M. and P.X. Ma, *3D nanofibrous scaffolds for tissue engineering.* Journal of Materials Chemistry, 2011. **21**(28): p. 10243.
32. Stratton, S., et al., *Bioactive polymeric scaffolds for tissue engineering.* Bioact Mater, 2016. **1**(2): p. 93-108.
33. Gerçek, I., R. Tığlı, and M. Gümüşderelioğlu, *A novel scaffold based on formation and agglomeration of PCL microbeads by freeze-drying.* Journal of Biomedical Materials Research Part A, 2008. **86**(4): p. 1012-1022.
34. Kazimoğlu, C., et al., *A novel biodegradable PCL film for tendon reconstruction: Achilles tendon defect model in rats.* The International journal of artificial organs, 2003. **26**(9): p. 804-812.
35. Alves da Silva, M., et al., *Cartilage tissue engineering using electrospun PCL nanofiber meshes and MSCs.* Biomacromolecules, 2010. **11**(12): p. 3228-3236.
36. Narayanan, G., B.S. Gupta, and A.E. Tonelli, *Enhanced mechanical properties of poly (ε-caprolactone) nanofibers produced by the addition of non-stoichiometric inclusion complexes of poly (ε-caprolactone) and α-cyclodextrin.* Polymer, 2015. **76**: p. 321-330.
37. Nada, A.A., et al., *A smart methodology to fabricate electrospun chitosan nanofiber matrices for regenerative engineering applications.* Polymers for Advanced Technologies, 2014. **25**(5): p. 507-515.
38. R.L. Kronenthal, Polymers in Medicine and Surgery, Springer, 1975, pp. 119e137.
39. Gentile, P., et al., *An overview of poly (lactic-co-glycolic) acid (PLGA)-based biomaterials for bone tissue engineering.* International journal of molecular sciences, 2014. **15**(3): p. 3640-3659.

40. Fisher, J.P., D. Dean, and A.G. Mikos, *Photocrosslinking characteristics and mechanical properties of diethyl fumarate/poly(propylene fumarate) biomaterials.* Biomaterials, 2002. **23**(22): p. 4333-4343.
41. P.Fisher, J., et al., *Synthesis and properties of photocross-linked poly(propylene fumarate) scaffolds.* Journal of Biomaterials Science, Polymer Edition, 2001. **12**(6): p. 673-687.
42. He, S., et al., *Synthesis of biodegradable poly (propylene fumarate) networks with poly (propylene fumarate)–diacrylate macromers as crosslinking agents and characterization of their degradation products.* Polymer, 2001. **42**(3): p. 1251-1260.
43. Pilipchuk, S.P., et al., *Tissue engineering for bone regeneration and osseointegration in the oral cavity.* Dent Mater, 2015. **31**(4): p. 317-38.

IX. Appendix

COPIES OF THE PUBLICATIONS PROVIDING THE BASIS OF THE THESIS

Excimer Laser-produced Biodegradable Photopolymer Scaffolds Do Not Induce Immune Rejection In Vivo

Balázs FARKAS[1, §], Adam ZSEDENYI[2, §], Edina GYUKITY-SEBESTYEN[3], Ilaria ROMANO[1], Katalin NAGY[2], Alberto DIASPRO[1], Fernando BRANDI[1,4], Krisztina BUZAS[2,3] and Szabolcs BEKE[1*]

[1]*Department of Nanophysics, Istituto Italiano di Tecnologia (IIT), Via Morego 30, 16163 Genova, Italy*
[2]*University of Szeged, Faculty of Dentistry, Tisza Lajos krt. 64. H-6720 Szeged, Hungary*
[3]*Hungarian Academy of Sciences, Biological Research Centre, Temesvari krt. 62, H-6726 Szeged, Hungary*
[4]*Istituto Nazionale di Ottica, Via Moruzzi 1, 56124-Pisa, Italy*

**Corresponding author's e-mail: szabolcs.beke@iit.it*

§ These authors equally contributed to the work

Following our previous works of in-vitro tests, the biocompatibility of photopolymer scaffolds was tested against immune responses *in vivo*. Neither relevant immune reactions nor the rejection of implanted scaffolds was detected, being an essential step for *in vivo* implantation of excimer laser-prepared scaffolds. The scaffolds were fabricated by UV excimer laser photocuring at 308 nm. After two weeks of transplantation neither inflammatory response nor reactive immune activation was detected based on the chemokine and cytokine profile. As a sign of biodegradability of the scaffolds, we detected macrophage infiltration and phagocytosis of the biopolymer at the site of implantation. Our results suggest that poly(propylene fumarate) (PPF): diethyl fumarate (DEF) (7 : 3 w/w) scaffolds have appropriate properties for *in vivo* applications.
DOI: 10.2961/jlmn.2015.01.0002

Keywords: excimer lasers, scaffold fabrication, biocompatibility; biodegradation; in vivo experiments

1. Introduction

One of the major goals of tissue engineering [1-2] is to provide rapid and reliable production of well-designed and functional microenvironments called scaffolds. These scaffolds help to reestablish the structural integrity of tissues damaged by trauma, disease or aging.

Our novel Mask Projection Excimer Stereolithography (MPExSL) [3] is a versatile and fast tool to fabricate such microenvironments from liquid polymeric resins through UV photocuring. Yet, the biocompatibility [4] of these scaffolds must also be one of the primary factors considered before the structures may be used in therapeutic applications.

The validity of poly(propylene fumarate) (PPF):diethyl fumarate (DEF) (7:3 w/w) samples fabricated by our MPExSL system has already been investigated by a previous study with bone cell culturing [5], while elastine [6-7] and Titanate nanotubes [8-9] were utilized as functional coatings. Following all these *in vitro* cell tests, *in vivo* biological testing of such PPF:DEF scaffolds became a fundamental aspect of our further progress.

2. Materials and Methods

2.1 Laser photocuring and setup

In MPExSL, schematically illustrated in Fig. 1, the image of a mask is projected on the photosensitive liquid resin [10] defining the inner geometry of the solidified polymer scaffold.

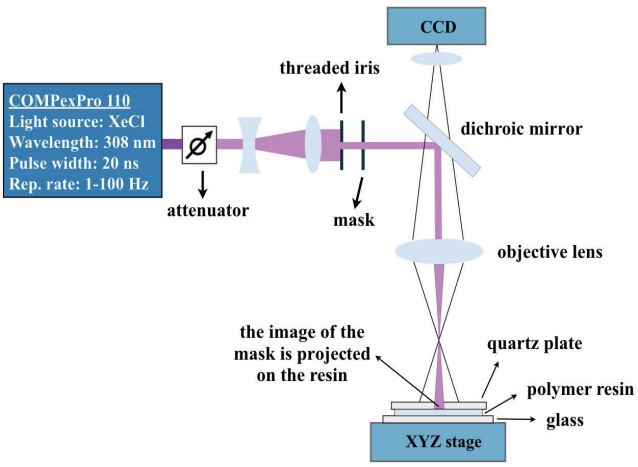

Fig. 1: MPExSL in a one-layer photocuring setup

The resin is sandwiched between a glass holder and a quartz plate [11], in favor of a simpler and faster one-layer photocuring process. The sample is then mounted on an XYZ stage.

The outer geometry can be modulated by an iris. Pulse fluence of the XeCl excimer laser is controlled by a variable attenuator. Pulse repetition rate ranges from 1 to 100 Hz. A CCD camera is mounted on the top of the optical system to in-situ monitor the process.

The system is entirely driven by a computer. Depending on the programming, this results in different scaffold geometries (as seen on Fig. 2) [3,5].

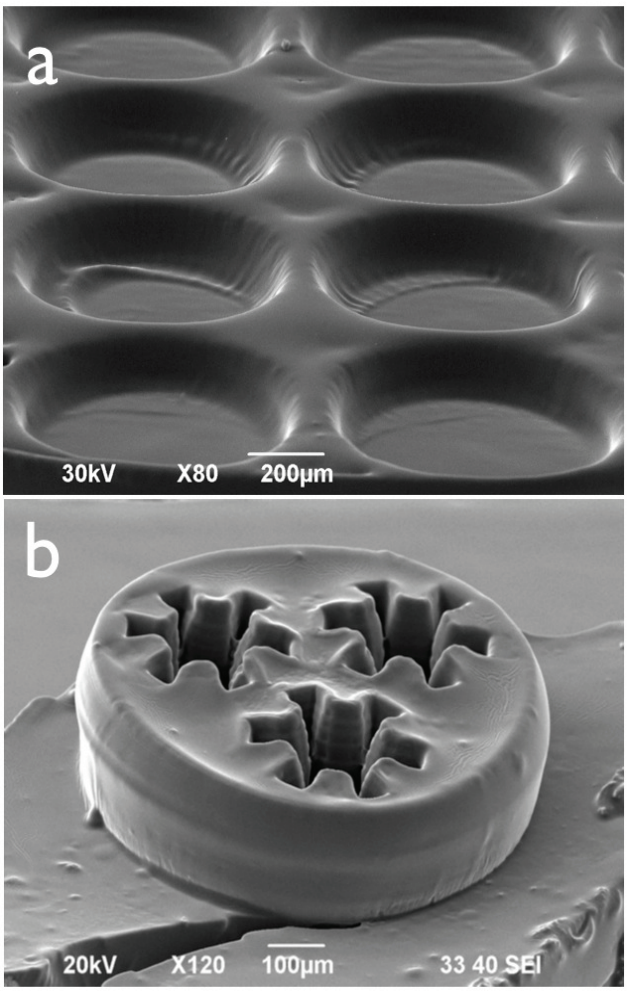

Fig. 2 (a) 5-mm diameter, 200-µm thick scaffold with pore size of 800 µm; **(b)** 2-mm diameter, 250-µm thick scaffold with cog-shaped pores

2.2 Polymer resin

Scaffolds fabricated from PPF:DEF (7:3 w/w) [11-12] were implanted. The structures were constructed by applying UV excimer laser photocuring at 308 nm. The photo-cross-linking density is tuned by photoinitiator phenylbis (2,4,6-trimethylbenzoyl) phosphine oxide (BaPO). Scaffold thickness can be adjusted by the total fluence (in this study by changing the number of shots). This tuning capability is discussed in section 3.1.

2.3 Biological testing: cell culture, mouse model, histology, and cytokine/chemokine profile

The photocured samples were sterilized with UV irradiation for 30 min and coated with 0.01 % poly-L-lysine (MW 70000-150000 Da, Sigma) for 30 min at room temperature. Poly-L-lysine was removed and the scaffolds were dried under laminar box, and then incubated in Eagle's Minimum Essential Medium (EMEM, Lonza) with 10 % fetal bovine serum, 100 U/ml penicillin, 100 U/ml streptomicin and 0.25 µg/µl fungizone (Promocell) for 7 days at 37 °C. The medium was changed every other day.

At day seven, K7M2 mouse cells (provided by Dennis Klinman, NCI-Frederick, MD, USA) were seeded in EMEM at 2 x 10^5 cells/ml in wells containing one scaffold each, and then incubated in humidified atmosphere with 5 % CO_2 at 37 °C for 14 days. After being covered with cells, the scaffolds were implanted under the dorsal skin of 8-week old female Balb/C mice (Charles River Laboratories International, Inc.). Control groups were implanted with cell-free scaffolds. 14 days after transplantation, the scaffolds and dorsal skin were removed and blood samples were collected. Five mice per group were implanted.

In case of a successful cell implantation, the presence or absence of selected K7M2 mouse osteosarcoma cell line was followed by histology. Specimens were fixed in 4% buffered paraformaldehyde and then embedded into paraffin blocks. Four-µm-thick sections were prepared and stained by conventional hematoxilin-eosin stain then coverslipped. The sections were visualized by scanning virtual microscope (3D Histech, Hungary).

The potential inflammatory reactions of the implanted biomaterial were screened via cytokine and chemokine profile. Protein concentrations of the sera were measured by BCA Protein Assay (Thermo Scientific) and pooled samples were tested to simultaneously detect relative levels of different cytokines according to the manufacture's instruction by Mouse Cytokine Array, Panel A (R&D Systems). Immunoreactive signals were detected using a LI-COR ODYSSEY® Fc (Dual-mode imaging system) imager followed by analysis with Odyssey v1.2 software. Animal care was provided in accordance with the procedures outlined in the animal protocol authorized by the Institutional and the National Animal Ethics and Experimentation Boards.

3. Results and discussion

3.1 Preliminary results for PPF:DEF (7:3 w/w) scaffold fabrication

The wavelength of a XeCL excimer laser (308 nm) has the greatest penetration depth of all excimer sources in PPF:DEF and thus highly desirable for the scaffold fabrication process [11]. Apart from the wavelength of the laser, the thickness of the polymerized layer can also be tuned by other laser parameters [13], such as the applied total fluence. The range of this tuning is strongly dependent on the resin's photoinitiator concentration. Thus, the layer thickness dependence over the BaPO (Fig. 3) was acquired for PPF:DEF (7:3 w/w) to be able to achieve the proper layer thickness of any desired structure.

For all measurements, non-porous layers were fabricated with different BaPO concentrations using a repetition

rate of 50 Hz and fluence per pulse of 20 mJ/cm^2. The applied numbers of pulses were 50, 124, 248, 336, 480, 720 and 1000. Height measurements were performed with a Veeco Dektak 150 profiler. BaPO concentration ranged from 0.3% to 1.2%. We assume that the observed sublinear dependence is due to the 308 nm light having greater penetration depth in the crosslinked resin than in the pristine one.

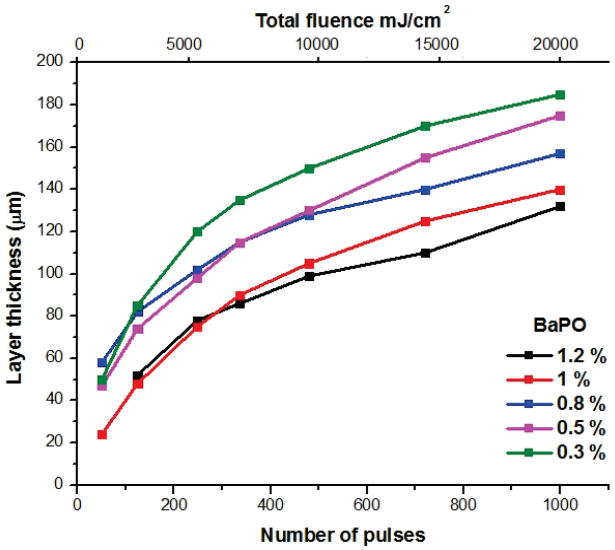

Fig. 3: Layer thickness as a function of number of pulses (and total fluence) in case of various BaPO concentrations

For the *in vivo* tests, 5-mm diameter, 100-µm thick porous scaffolds were prepared with 55-µm-pore diameters, using a BaPO concentration of 1%. These have been presented in [9].

3.2 In-vivo biocompatibility of monolayer scaffolds

K7M2 mouse osteosarcoma cell line was grown on the scaffolds for 14 days before implantation in mice. The control group was implanted with cell-free scaffolds. After 14 days, the scaffolds and dorsal skin were removed and serum samples were harvested for further analysis.

Cytokine and chemokine protein levels in sera were also investigated. No significant difference was detected between the cytokine profiles of the tumor scaffold implanted group and the control group (Fig 4). No sign of inflammation was observed on the dorsal skin: neither inflammatory cytokines, nor other signs of rejective reaction were found.

In histological sections (Fig. 5) of the group implanted with tumor seeded scaffolds (b), viable anaplastic sarcomatous tumor cells embedded in dens inflammatory reaction were seen (d-interrupted line indicates tumor border), in contrast to the control group (a) where only a mild fibrotic reaction was noted around the presumable location of the scaffold (Fig 8c-arrows).

No residual biopolymer piece was found in the control animals. We presume that the scaffolds degraded biologically *in vivo* without significant residual pieces**.**

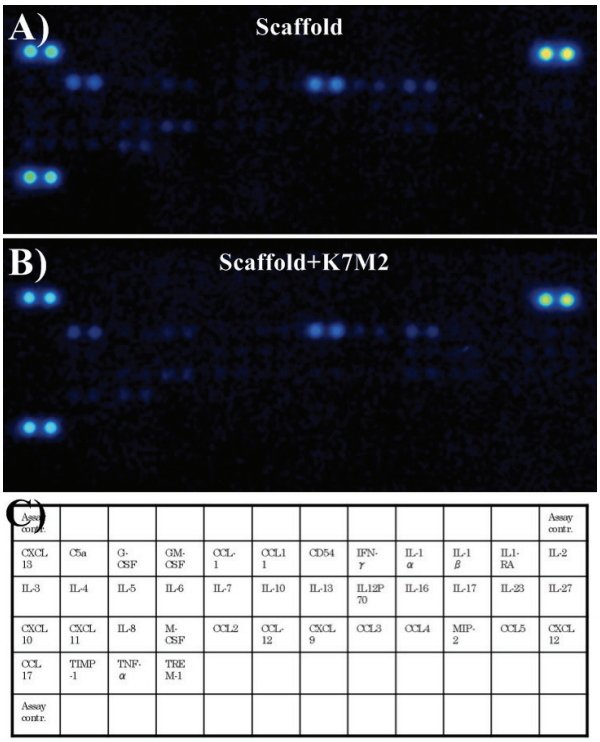

Fig. 4: profiling of (A) tumor scaffold implanted mice sera and (B) control groups sera. Panel (C) shows the cytokine and chemokine map

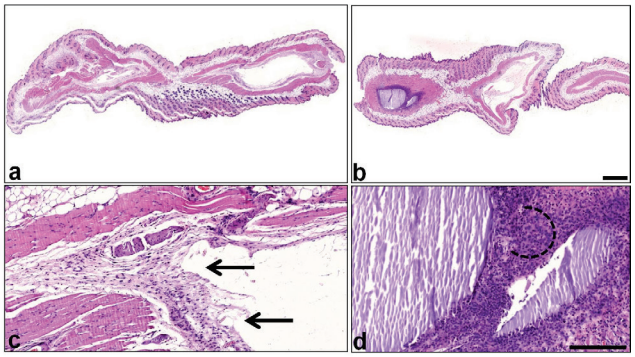

Fig. 5: HE; OM 200x; a-b and c-d scale bar 1000 µm and 200 µm, respectively

Conclusions

PPF:DEF scaffolds were fabricated by our excimer laser stereolithography system and have been tested *in vivo* with K7M2 mouse osteosarcoma cell line. No inflammatory reaction or other rejection was observed opening up the possibility of utilizing the aforementioned scaffolds in biological applications, while the MPExSL presents a fast, versatile, and reliable way to fabricate simple photocured structures for tissue engineering and regenerative medicine.

Acknowledgments and Appendixes

This work has received funding support from the European Union (FP7-NMP-2013-EU-China) grant agreement n.604263 (NEUROSCAFFOLDS) and the grant of The Hungarian Social Renewal Operational Program (TAMOP-4.2.2-A-11/1/KONV-2012-0025). The project is co-financed by the European Union and the European Social Fund.

References

[1] R. Langer and J. P. Vacanti, „Tissue engineering", Science 260, 920-926 (1993)

[2] Tabata, Y., „Biomaterial technology for tissue engineering applications", J. R. Soc. Interface 6, S311–S324 (2009)

[3] S. Beke, B. Farkas, I. Romano, F. Brandi, „ 3D scaffold fabrication by Mask Projection Excimer laser Stereolithography", Vol. 4, Issue 10, pp. 2032-2041 (2014), http://dx.doi.org/10.1364/OME.4.002032

[4] Williams, D. F., „The Williams dictionary of biomaterials", Liverpool, UK: University Press (1999)

[5] S Beke, F Anjum, H Tsushima, L Ceseracciu, E Chieregatti, A Diaspro, A. Athanassiou, F. Brandi, „Towards excimer-laser-based stereolithography: a rapid process to fabricate rigid biodegradable photopolymer scaffolds", Journal of The Royal Society Interface 9 (76), 3017-3026 (2012), http://dx.doi.org/10.1098/rsif.2012.0300

[6] S Scaglione, R Barenghi, S Beke, L Ceseracciu, I Romano, F Sbrana, P. Stagnaro, F. Brandi, M. Vassalli, „Characterization of bioinspired elastin-polypropylene fumerate material for vascular prostheses applications", SPIE Optical Metrology, 87920H-87920H-6 (2013) http://dx.doi.org/10.1117/12.2021754

[7] R. Barenghi, S. Beke, I. Romano, P. Gavazzo, F. Sbrana, M. Vassalli, F. Brandi, S. Scaglione „Elastin-coated biodegradable photopolymer scaffolds for enhanced cell adhesion and proliferation" BioMed Research International, vol. 2014, Article ID 624645, 9 pages, (2014). http://dx.doi.org/10.1155/2014/624645

[8] S Beke, L Kőrösi, A Scarpellini, F Anjum, F Brandi, „Titanate nanotube coatings on biodegradable photopolymer scaffolds", Materials Science and Engineering: C 33, Pages 2460–2463 (2013), http://dx.doi.org/10.1016/j.msec.2013.01.066

[9] S. Beke, R. Barenghi, B. Farkas, I. Romano, L. Kőrösi, S. Scaglione, F. Brandi, „Improved cell activity on biodegradable photopolymer scaffolds using titanate nanotube coatings" Materials Science and Engineering C, 44, 38-43, (2014), http://dx.doi.org/10.1016/j.msec.2014.07.008

[10] Ha, Y. M., Choi, J. W. & Lee, S. H. „Mass production of 3-D microstructures using projection microstereolithography", J. Mech. Sci. Technol. 22, 514–521 (2008)

[11] S Beke, F Anjum, L Ceseracciu, I Romano, A Athanassiou, A Diaspro, F Brandi, „Rapid fabrication of rigid biodegradable scaffolds by excimer laser mask projection technique: a comparison between 248 and 308 nm", Laser Physics 23 (3), 035602, (2013), doi:10.1088/1054-660X/23/3/035602

[12] Kasper, K. F., Tanahashi, K., Fisher, J. P. & Mikos, A. G., „Synthesis of poly(propylene fumarate)", Nat. Protocol 4, 518–525. (2009)

[13] B. Farkas, I. Romano, L. Ceseracciu, A. Diaspro, F. Brandi, S. Beke, "Four-order stiffness variation of laser-fabricated photopolymer biodegradable scaffolds by laser parameters modulation", Materials Science and Engineering: C, 2015

(Received:July 18, 2014, Accepted: November 23, 2014)

Materials Science and Engineering C 72 (2017) 625–630

Contents lists available at ScienceDirect

Materials Science and Engineering C

journal homepage: www.elsevier.com/locate/msec

Gold nanoparticle-filled biodegradable photopolymer scaffolds induced muscle remodeling: *in vitro* and *in vivo* findings

Adam Zsedenyi [a], Balazs Farkas [b], Gaser N. Abdelrasoul [b], Ilaria Romano [b], Edina Gyukity-Sebestyen [c], Katalin Nagy [a], Maria Harmati [c], Gabriella Dobra [c], Sandor Kormondi [d], Gabor Decsi [a], Istvan Balazs Nemeth [e], Alberto Diaspro [b], Fernando Brandi [b,f], Szabolcs Beke [b], Krisztina Buzas [a,c,g,*]

[a] University of Szeged, Faculty of Dentistry, Tisza Lajos krt. 64, H-6720 Szeged, Hungary
[b] Department of Nanophysics, Istituto Italiano di Tecnologia (IIT), Via Morego 30, 16163 Genova, Italy
[c] Hungarian Academy of Sciences, Biological Research Centre, Temesvari krt. 62, H-67268 Szeged, Hungary
[d] University of Szeged, Department of Traumatology, Semmelweis utca 6, H-6720 Szeged, Hungary
[e] University of Szeged, Department of Dermatology and Allergology, Koranyi fasor 6, H-6720 Szeged, Hungary
[f] Istituto Nazionale di Ottica (INO-CNR), Via Moruzzi 1, 56124 Pisa, Italy
[g] Biological Research Centre Institute of Biochemistry H-6726 Szeged, Temesvari krt. 62. Hungary

ARTICLE INFO

Article history:
Received 15 August 2016
Accepted 27 November 2016
Available online 2 December 2016

ABSTRACT

Therapeutic stem cell transplantation bears the promise of new directions in organ and tissue replacement, but a number of its difficulties and perils are also well known. Our goal was to develop a method of transplantation by which the transplanted cells remain confined to the transplantation site and induce favorable processes. With the help of mask-projection excimer laser stereolithography, 3D hybrid nanoscaffolds were fabricated from biodegradable, photocurable PPF:DEF resin with incorporated gold nanoparticles (Au NPs). The scaffolds were tested *in vitro* and *in vivo* in order to find out about their biocompatibility and fitness for our purposes.

In vitro, macrophages and mouse autologous adipose stem cells (ASCs) were seeded over the hybrid scaffolds and non-hybrid (with Au NPs) scaffolds for 4 days. The hybrid nanocomposite greater stem cell dispension and stem cell adhesion than PPF scaffolds without Au NPs, but such a difference was not seen in the case of macrophages. *In vivo*, stem cells, scaffoldings and scaffoldings covered in stem cells were transplanted under the back skin of mice. After 14 days, blood samples were taken and the affected skin area was excised. Cytokine and chemokine profiling did not indicate elevated immunomediators in the sera of experimental animals. Interestingly, the autologous-stem-cell-seeded hybrid nanocomposite scaffold induced muscle tissue regeneration after experimental wound generation *in vivo*. We could not observe such stem cell-induced tissue regeneration when no scaffolding was used.

We conclude that PPF:DEF resin nanoscaffolds with incorporated gold nanoparticles offer a safe and efficient alternative for the enhancement of local tissue remodeling. The results also support the idea that adipose derived stem cells are an optimal cell type for the purposes of regenerative musculoskeletal tissue engineering.

1. Introduction

Tissue Engineering (TE) is one of the most progressively developing disciplines [1–3], the development of which is largely stimulated by its biomedical potential. Throughout the last decade, various health issues have been successfully addressed utilizing a TE approach, such as bone regeneration [4] bladder [5] and muscle [6,7] augmentation/repair and also neuroregeneration [8,9].

The utility of polypropylene fumarate (PPF):diethyl fumarate (DEF) (7:3 w/w) biodegradable photocurable polymers in TE has already been widely investigated [10,11]. The results were promising, but further *in vivo* corroboration is still lacking.

Mask projection excimer laser stereolithography (MPExSL) [12] makes it possible to fabricate 3D scaffolds in the nano range, including PPF:DEF nanocomposite scaffolds [13]. Such scaffolds act as a template for cell organization and tissue development in the tissue engineering process, and they are also biodegradable. Furthermore, to augment their efficiency, hybrid scaffolds can be fabricated by incorporating nanoparticles into the polymer resin, as recently reported by our group using [14] and gold [13] nanoparticles. The optical and physicochemical properties of Au NPs have been intensively investigated,

* Corresponding author at: University of Szeged, Faculty of Dentistry, Tisza Lajos krt. 64, H-6720 Szeged, Hungary.
E-mail address: kr.buzas@gmail.com (K. Buzas).

http://dx.doi.org/10.1016/j.msec.2016.11.124
0928-4931/

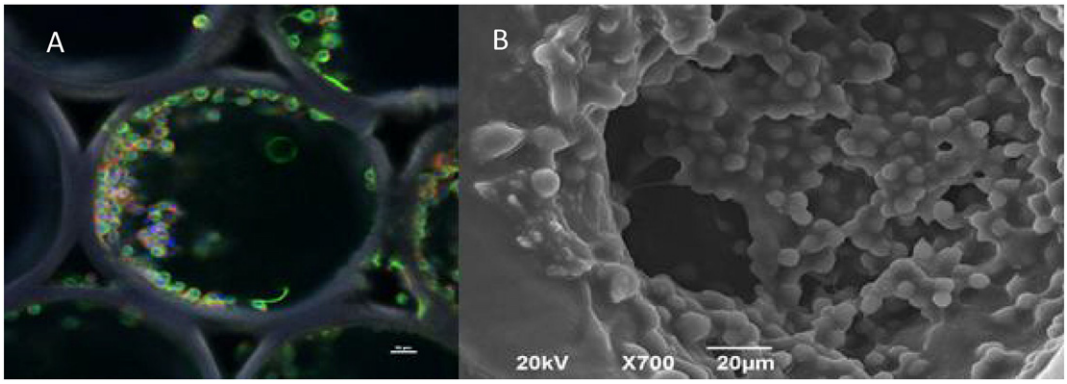

Fig. 1. Scaffold of 200 μm pore size, with Au nanoparticles and macrophages A) confocal microscopy, B) SEM.

along with their potential biomedical uses. Au NPs appear to be optimal candidates to be used as "transport vehicles" in scaffolds, due to their low inherent toxicity, tunable stability, switchable plasmonic optical properties and high surface area [15].

In this study, we conducted *in vitro* and *in vivo* experiments. The aim of our *in vitro* experiment was to investigate the interactions of the biodegradable Au NP hybrid scaffold with the adhesion and proliferation of mouse autologous adipose stem cells (ASCs) and macrophages as compared to non-hybrid PPF:DEF scaffolds.

In vitro, two different cell lines were used for the testing of the scaffolds. One of these, RAW 264.7, is a macrophage cell line of good proliferative potential and excellent adherence. In the other case, a primary cell culture also fit for real transplantation purposes was used (ASCs). In comparison with transformed cell lines, the adherence and proliferative potential of these cells is less well-defined. This way it was possible to test the biocompatibility of the scaffolds with both a stable and a sensitive system. During the *in vitro* experiments we managed to optimize the conditions for the proliferation and adherence of the stem cells.

The aim of the *in vivo* part of the study was to provide further support for our previous findings regarding the favorable biocompatibility of these scaffolds [13] - this time with the Au NP hybrids. To reach that end, stem cells, scaffoldings and scaffoldings covered in stem cells were transplanted under the back skin of mice. Inflammatory and allergic reactions upon transplantation are among the first signs of impending failure. The measurement of inflammatory cytokine and chemokine levels allows a sensitive detection of such processes, wherefore we utilized a proteome profiler capable of detecting 44 cytokines and chemokines.

The cytokine and chemokine profiling was followed by the histological analysis of the removed implant, which was important in two ways. First, histology verified the biodegradability of the polymer. Second, this way we could rule out tumor formation, which is a potential and dangerous side effect of stem cell transplantation. Finally, the results of the immunological profiling could be verified by the lack of inflammatory infiltration.

Interestingly, the autologous-stem-cell-seeded hybrid nanocomposite scaffold induced muscle tissue regeneration after experimental wound generation *in vivo*.

2. Materials and methods

2.1. Mask-projection excimer laser stereolithography (MPExSL)

MPExSL is a stereolithography process developed in our laboratory [15] based on excimer laser irradiation of a liquid photocrosslinkable resin. The geometry and physical properties of the scaffolds to be fabricated is selected by a set of interchangeable masks and different laser and resin parameters, such as the laser wavelength [15], number of laser pulses and/or pulse fluence [16,17], and the photoinitiator concentration [15]. The setup is described in detail in Beke et al. [15].

2.2. Polymer resin

The PPF:DED biodegradable photopolymer resin preparation is described in detail in our previous work [18]. The preparation of PPD:DEF–Au NP nanocomposites is described previously [13].

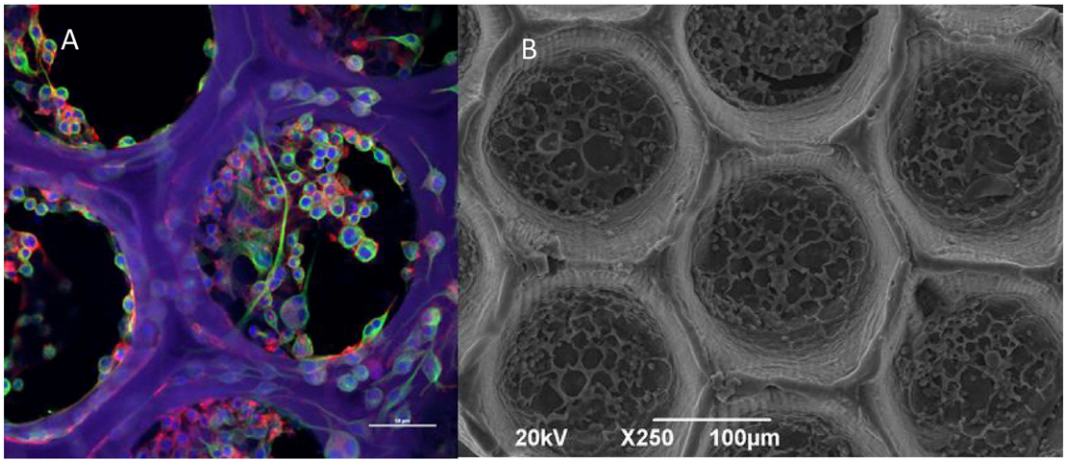

Fig. 2. Scaffold of 200 μm pore size, without Au nanoparticles and macrophages A) confocal microscopy, B) SEM.

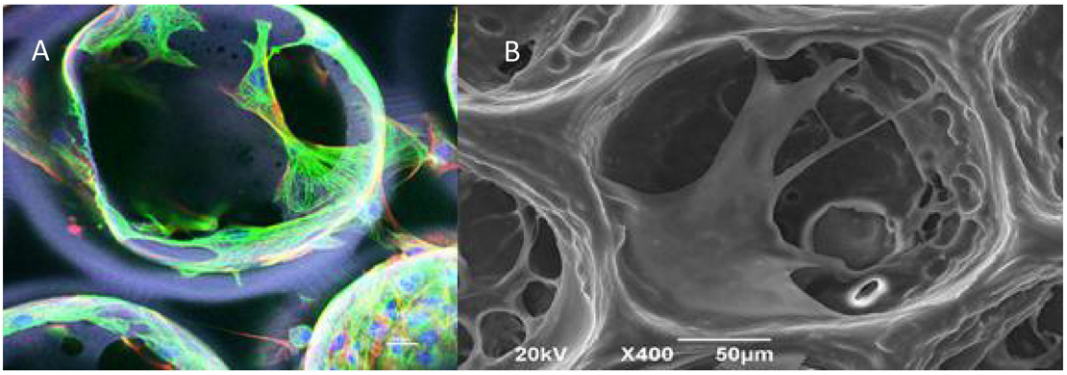

Fig. 3. Scaffold of 200 μm pore size, with Au nanoparticles and with mouse ASCs A) confocal, B) SEM.

To test the produced Au nanocomposite scaffolds, we used biodegradable scaffolds with 200 μm pore size and 5.52 μM Au nanoparticle [13].

2.3. Biological testing: cell culture, mouse model, histology, and cytokine/chemokine profile

The primary autologous adipose stem cells were isolated from 4 to 6 weeks old Balb/c mice (Charles River Laboratories International, Inc.). After cervical dislocation, the abdominal adipose tissue was removed. The tissue was put in 100 μg/ml RPMI (Lonza, Cat. No.: BE12-115F) treated with kanamycin (Kanamycin sulfate from Streptomyces Kanamyceticus, Sigma K 1377-16), then digested in collagenase (Sigma) at 37 °C. After 1 h, the cells were washed and cultured in a Petri dish for 2 weeks in MSC Medium (MesenCult, STEMCELL) with 10% fetal bovine serum, 100 U/ml penicillin, 100 U/ml streptomycin and 0.25 μg/μl fungizone (Promocell) at 37 °C, 5% CO_2.

2.3.1. In vitro experiments

The photocured samples were sterilized with UV irradiation for 30 min and coated with 0.01% poly-Llysine (MW 70,000–150,000 Da, Sigma) for 30 min at room temperature. Poly-L-lysine was removed and the scaffolds were dried under laminar box, and then incubated in Eagle's Minimum Essential Medium (EMEM, Lonza) with 10% fetal bovine serum, 100 U/ml penicillin, 100 U/ml streptomycin and 0.25 μg/μl fungizone (Promocell) for 7 days at 37 °C. At day seven, adipose-derived mesenchymal stem cells (ASC) isolated from Balb/c male mouse or macrophages (RAW 264.7) were seeded at 7×10^4 cells/ml in wells containing one scaffold each, and then incubated in humidified atmosphere with 5% CO_2 at 37 °C for 4 days. Cell-seeded-scaffolds with cells were prepared for Scanning Electron Microscope (SEM), and Confocal microscope (Nikon A1) examination. For the preparation for Confocal microscopy we used 4% paraformaldehyde and immune staining (Alpha tubulin, Phalloidin, Dapi). SEM samples were treated 0.1 M Sodium Cacodylate, and 1.2% Glutaraldehyde. Samples were dehydrated in ethanol of increasing concentration (50%, 70%, 80%, 90%, 96%, 100%) for 10 min each concentration and 100% Hexamethyldisilazane overnight.

2.3.2. In vivo experiments

The MPExSL-fabricated samples were sterilized with UV irradiation for 30 min and coated with 0.01% poly-L-lysine (MW 70,000–150,000 Da, Sigma) for 30 min at room temperature. Poly-L-lysine was removed and the scaffolds were dried under laminar box, and then incubated in Eagle's Minimum Essential Medium (EMEM, Lonza) with 10% fetal bovine serum, 100 U/ml penicillin, 100 U/ml streptomycin and 0.25 μg/μl fungizone (Promocell) for 7 days at 37 °C. The medium was changed every other day. At day seven, ASCs were seeded in MSC Medium at 5×10^4 cells/ml in wells containing one scaffold each, and then incubated in humidified atmosphere with 5% CO_2 at 37 °C for 7 days. After being covered with cells, the scaffolds were implanted

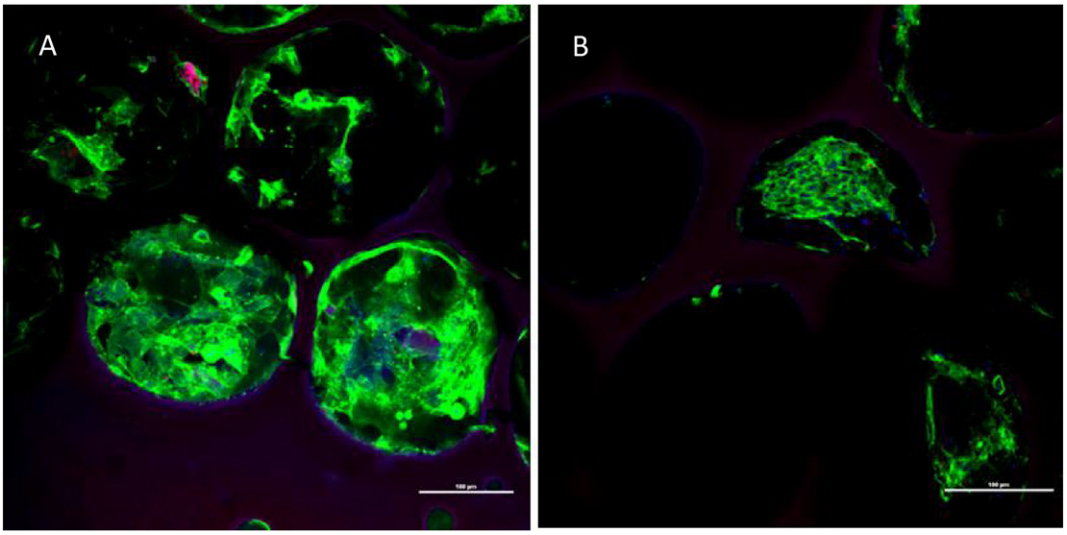

Fig. 4. ASC adhesion to a hybrid (A) and a normal (B) scaffold.

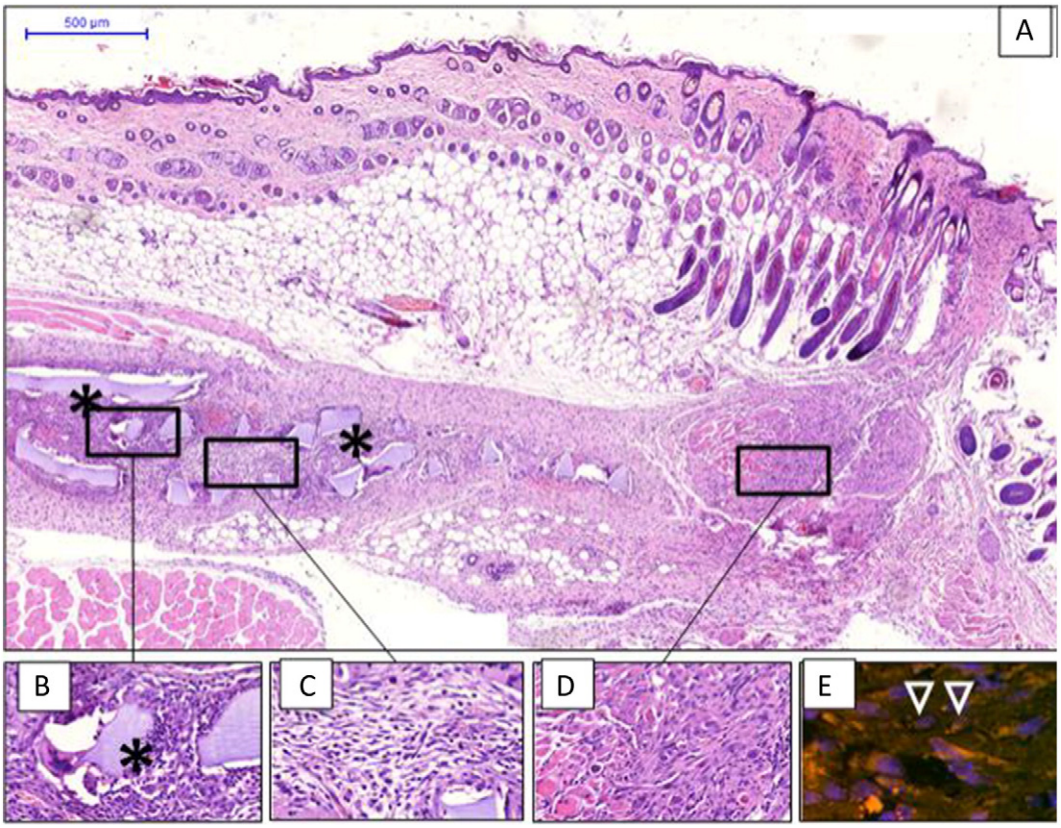

Fig. 5. Images of a section with ASC seeded Au filled scaffold (A, B, C). Viable mesenchymal cell colonies and striated muscle regeneration indicated by stem cells were seen in the scaffold specimen (D). The Y chromosome content of the transplanted stem cells was detected by the FISH technique, red dots indicated by arrowheads (E).

under the dorsal skin of 8 week old female Balb/c mice (Charles River Laboratories International, Inc.). The control group was injected with 5×10^4 ASCs. Three mice per group were implanted. 14 days after transplantation, the scaffolds and dorsal skin were removed and blood samples were collected. For cytokine and chemokine profile, collected blood samples were allowed to clot for 30 min at room temperature, then overnight at 4 °C. Serum samples were collected by centrifugation at 3000 rpm for 5 min and stored at −80 °C until the time of analysis. In case of a successful cell implantation, the presence or absence of selected mouse ASC was followed by histology. Specimens were fixed in 4% buffered paraformaldehyde and then embedded in paraffin blocks. Four-micrometer-thick sections were prepared and stained by conventional hematoxylin-eosin stain then coverslipped. The sections were visualized by scanning virtual microscope (3D Histech, Hungary). Inflammatory reactions were detected by cytokine and chemokine profiling.

Protein concentrations of the sera were measured by BCA Protein Assay (Thermo Scientific) and pooled samples were tested to simultaneously detect relative levels of different cytokines according to the manufacturer's instructions by Mouse Cytokine Array, Panel A (R&D Systems). Immunoreactive signals were detected using an LI-COR ODYSSEY Fc imager followed by analysis with Odyssey v1.2 software. All animal experiments were performed in accordance with national (1998. XXVIII; 40/2013) and European (2010/63/EU) animal ethics guidelines. The experimental protocols were approved by the Animal Experimentation and Ethics Committee of the Biological Research Centre of the Hungarian Academy of Sciences and the Hungarian National Animal Experimentation and Ethics Board (clearance number: XVI./03521/2011.)

For fluorescence *in situ* hybridization (FISH), chromosome X and Y control probe (Empire Genomics, Buffalo, NY, USA) was used to verify the presence of the Y chromosome of the transplanted mouse adipose stem cells, according to the manufacturer's instructions.

3. Results

3.1. In vitro tests

Macrophages –a cell type of high adherence-could be seeded on the scaffold surface as shown in Fig. 1.

The Au-content of the polymer resin had no influence on the adherence of the macrophages (Fig. 2).

The adherence of ASCs, however, proved to be sensitive to the Au content. Adherence to the Au NP hybrid scaffold proved to be much better (Figs. 3, 4).

3.2. In vivo tests

The excised skin areas showed no visible signs of reactive inflammation (Fig. 5), and the cytokine profiling did not indicate inflammation either (Fig. 6).

Interestingly, we detected not only the implanted ASCs with X-Y chromosome but also cells containing Y and more than one X chromosomes, most likely resulting from regenerative cellular fusion between ASCs and stromal mesenchymal cells (Fig. 5A). This suggests that the biopolymers applied together with ASCs were able to initiate tissue repair in the appropriate tissue environment.

We could not detect ASC or ASC-derived tissue regeneration in ASC injected mice when scaffold support was not utilized (data not shown). In the histological sections of the group implanted with adipose stem cells, small residual biopolymer pieces of varying diameter (50–500 μm) were seen.

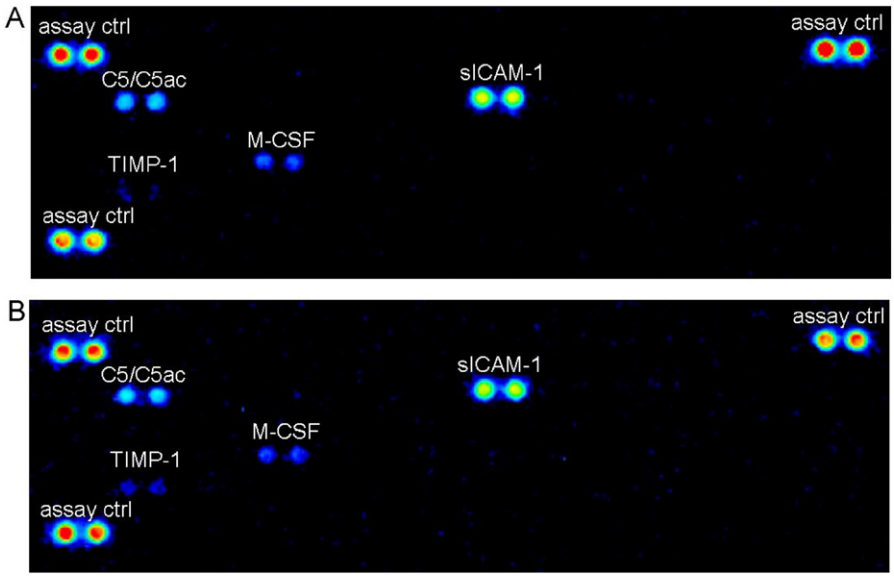

Fig. 6. Cytokine and chemokine proteome profiling detected C5 complement component, sICAM-1 adhesion molecule, M-CSF and TIMP-1 cytokines. The profiler did not indicate significant immune reaction to the ASC-seeded scaffolds (A) as compared to the control scaffold (B). This is supported by the lack of immune cell infiltration or relevant immune reaction against the ASC-seeded scaffold, as revealed by histology.

4. Conclusion

To use stem cells in the regenerative medicine is one of the most important challenge of tissue engineering. Stem cell implantation is the best way to regenerate different types of tissues based on pluripotency but the stem cells incorporated to the circulation could initiate cancerous transformation.

Biodegradable, photocurable polymer resin, polypropylene fumarate (PPF) along with Au NPs were utilized to synthesize a hybrid nanocomposite resin, that is directly exploitable in stereolithography (SL) processes. The resulting resin was used to fabricate nanocomposite scaffolds *via* mask projection excimer laser stereolithography.

In vitro studies helped to optimize scaffold structure, composition and cell culturing conditions for further *in vivo* experiments. We compared the colony-forming abilities of macrophages- as a highly adherent cell line- and the primary stem cell culture on different biomaterials. While the stable but transformed macrophage cell line was not especially sensitive to the Au-content of the polymer, the adherence and distribution of ASCs was definitely better on the Au hybrid polymer. This is important because of the potential value of these cells in regenerative tissue engineering.

Our results suggested to use Au-filled scaffolds to secure the optimal cell transfer. In the case of Au-filled scaffolds we have seen evenly distribution and adherence of stem cells.

As the potentially most dangerous sequela of the implantation of any foreign body is a violent immune response, monitoring immune reactions is of key importance. Neither immunological profiling nor histology revealed any sign of inflammatory or allergic reactions in our experimental animals. To our knowledge, we are the first to have proven that PPF:DEF Au NP scaffolds do not induce immune response in experimental animals.

These scaffolds provided an optimal surface for the adherence of ASCs and kept them in place, but an even more valuable observation was also made: ASCs induced muscle regeneration *in situ*, which was verified by the histological analysis and the FISH test. This in itself may not be new, as several publications have dealt with scaffold-derived muscle regeneration, but the preference of ASCs for this unique surface [13] make the Au NP nanocomposite- ASC system a really promising one for clinical applications.

Tumor formation is an ever-present danger of stem cell transplantation [19,20], but our system proved to be safe in this respect. The use of the scaffold ensures that the cells are kept in place, and the chance of stem cells getting into the bloodstream is significantly reduced. The use of autologous stem cells reduces the risk of rejection [21], ensures better regeneration [22], and ASCs are readily available. ASCs are easy to harvest in a safe, minimally invasive way from almost any patient.

We conclude that PPF:DEF resin scaffolds with incorporated gold nanoparticles, especially in combination with ASCs carry the promise of a new, safe and efficient means of musculoskeletal tissue regeneration [2].

Acknowledgement

This research was funded by Hungarian Scientific Research Fund (OTKA K) 112493 and GINOP-2.3.2-15-2016-00001.

The authors would like to thank Gábor Braunitzer for his helpful comments.

References

[1] H.T. Liao, C.T. Chen, Osteogenic potential: comparison between bone marrow and adipose-derived mesenchymal stem cells, World. J. Stem. Cells. 6 (3) (2014) 288–295, http://dx.doi.org/10.4252/wjsc.v6.i3.288.
[2] A. Trumbull, G. Subramanian, E. Yildirim-Ayan, Mechanoresponsive musculoskeletal tissue differentiation of adipose-derived stem cells, Biomed. Eng. Online 15 (2016) 43, http://dx.doi.org/10.1186/s12938-016-0150-9.
[3] R. Langer, J.P. Vacanti, Tissue engineering, Science 260 (1993) 920–926, http://dx.doi.org/10.1126/science.8493529.
[4] A.M. Yousefi, P.F. James, R. Akbarzadeh, A. Subramanian, C. Flavin, H. Oudadesse, Prospect of stem cells in bone tissue engineering: a review stem, Cells. Int. (2016), Article ID 6180487. http://dx.doi.org/10.1155/2016/6180487 (13 pages).
[5] O. Lam Van Ba, S. Aharony, O. Loutochin, J. Corcos, Bladder tissue engineering: a literature review, Adv. Drug Deliv. Rev. 82–83 (2015) 31–37, http://dx.doi.org/10.1016/j.addr.2014.11.013.
[6] J.M. Grasman, M.J. Zayas, R.L. Page, G.D. Pins, Biomimetic scaffolds for regeneration of volumetric muscle loss in skeletal muscle injuries, Acta Biomater. 25 (2015) 2–15, http://dx.doi.org/10.1016/j.actbio.2015.07.038.
[7] J. Stern-Straeter, F. Riedel, G. Bran, K. Hörmann, U.R. Goessler, Advances in skeletal muscle tissue engineering, In Vivo. 21 (2007) 435–444.
[8] A. Faroni, S.A. Mobasseri, P.J. Kingham, A.J. Reid, Peripheral nerve regeneration: experimental strategies and future perspectives, Adv. Drug Deliv. Rev. 82–83 (2015) 160–167, http://dx.doi.org/10.1016/j.addr.2014.11.010.
[9] V. Chiono, C. Tonda-Turo, Trends in the design of nerve guidance channels in peripheral nerve tissue engineering, Prog. Neurobiol. 131 (2015) 87–104, http://dx.doi.org/10.1016/j.pneurobio.2015.06.001.
[10] J.W. Lee, K.S. Kang, S.H. Lee, J.Y. Kim, B.K. Lee, D.W. Cho, Bone regeneration using a microstereolithography-produced customized poly (propylene fumarate)/diethyl

fumarate photopolymer 3D scaffold incorporating BMP-2 loaded PLGA microspheres, Biomaterials 32 (2011) 744e752, http://dx.doi.org/10.1016/j.biomaterials.2010.09.035.
[11] P.X. Lan, J.W. Lee, Y.J. Seol, D.W. Cho, Development of 3D PPF/DEF scaffolds using micro-stereolithography and surface modification, J. Mater. Sci. Mater. Med. 20 (2009) 271–279, http://dx.doi.org/10.1007/s10856-008-3567-2.
[12] B. Farkas, A. Zsedenyi, E. Gyukity-Sebestyen, I. Romano, K. Nagy, A. Diaspro, F.K. Brandi, K. Buzas, S. Beke, Excimer laser-produced biodegradable photopolymer scaffolds do not induce immune rejection in vivo, JLMN 10 (2015) 11–14, http://dx.doi.org/10.2961/jlmn.2015.01.0002.
[13] G.N. Abdelrasoul, B. Farkas, I. Romano, A. Diaspro, S. Beke, Nanocomposite scaffold fabrication by incorporating gold nanoparticles into biodegradable polymer matrix: synthesis, characterization, and photothermal effect, Mater. Sci. Eng. C Mater. Biol. Appl. 56 (2015) 305–310, http://dx.doi.org/10.1016/j.msec.2015.06.037.
[14] B. Farkas, M. Rodio, I. Romano, A. Diaspro, R. Intartaglia, S. Beke, Fabrication of hybrid nanocomposite scaffolds by incorporating ligand-free hydroxyapatite nanoparticles into biodegradable polymer scaffolds and release studies, Beilstein. J. Nanotechnol. 6 (2015) 2217–2223, http://dx.doi.org/10.3762/bjnano.6.227.
[15] S. Beke, B. Farkas, I. Romano, F. Brandi, 3D scaffold fabrication by mask projection excimer laser stereolithography, Opt. Mater. Express. 4 (2014) 2032–2041, http://dx.doi.org/10.1364/OME.4.002032.
[16] S. Beke, F. Anjum, L. Ceseracciu, I. Romano, A. Athanassiou, A. Diaspro, F. Brandi, Rapid fabrication of rigid biodegradable scaffolds by excimer laser mask projection technique: a comparison between 248 and 308 nm, Laser Phys. 23 (3) (2013) 035602https://www.researchgate.net/publication/257416197.
[17] B. Farkas, I. Romano, L. Ceseracciu, A. Diaspro, F. Brandi, S. Beke, Four-order stiffness variation of laser-fabricated photopolymerbiodegradable scaffolds by laser parameter modulation, Mater. Sci. Eng. C Mater. Biol. Appl. 55 (2015) 14–21, http://dx.doi.org/10.1016/j.msec.2015.05.0540928-493.
[18] S. Beke, F. Anjum, H. Tsushima, L. Ceseracciu, E. Chieregatti, A. Diaspro, A. Athanassiou, F. Brandi, Towards excimer-laser-based stereolithography: a rapid process to fabricate rigid biodegradable photopolymer scaffolds, J. R. Soc. Interface 9 (2012) 3017–3026, http://dx.doi.org/10.1098/rsif.2012.0300.
[19] H.C. Li, C. Stoicov, A.B. Rogers, J. Houghton, Stem cells and cancer: evidence for bone marrow stem cells in epithelial cancers, World J. Gastroenterol. 12 (3) (2006) 363–371, http://dx.doi.org/10.3748/wjg.v12.i3.363.
[20] T.E. Werbowetski-Ogilvie, M. Bossé, M. Stewart, A. Schnerch, V. Ramos-Mejia, A. Rouleau, T. Wynder, M.J. Smith, S. Dingwall, T. Carter, C. Williams, C. Harris, J. Dolling, C. Wynder, D. Boreham, M. Bhatia, Characterization of human embryonic stem cells with features of neoplastic progression, Nat. Biotechnol. 27 (2009) 91–97, http://dx.doi.org/10.1038/nbt.1516.
[21] L.A. Vonk, T.S. de Windt, I.C. Slaper-Cortenbach, D.B. Saris, Autologous, allogeneic, induced pluripotent stem cell or a combination stem cell therapy? Where are we headed in cartilage repair and why: a concise review, Stem. Cell Res. Ther. 6 (2015) 94, http://dx.doi.org/10.1186/s13287-015-0086-1.
[22] D. Currò, G. Mancardi, Autologous hematopoietic stem cell transplantation in multiple sclerosis: 20 years of experience, Neurol. Sci. 37 (2016) 857–865, http://dx.doi.org/10.1007/s10072-016-2564-3.